Spatiotemporal profiling of neural crest cells in the common wall lizard *Podarcis muralis*

Robin Pranter[1] (https://orcid.org/0000-0003-3615-0281) and Nathalie Feiner[1]

[1]Department of Biology, Lund University, Sweden

Corresponding authors: robin.pranter@biol.lu.se, +46738413877 and nathalie.feiner@biol.lu.se

Running title: Neural crest cells in common wall lizards

Key words: Gene expression patterns, cell migration, cell differentiation, comparative embryology, squamate reptiles, HNK-1

Data availability statement: Not applicable.

Funding statement: This work was supported by Kungliga Fysiografiska Sällskapet i Lund (42010), Jörgen Lindströms stipendiefond to RP, and by the European Research Council (948126), and Swedish Research Council (2020-03650) to NF.

Conflict of interest disclosure: The authors of this study declare no conflicts of interest.

Ethics approval statement: The embryos were collected from eggs laid by animals kept under breading permit 5.2.18-10993/18 granted by the Swedish ministry of agriculture.

Patient consent statement: Not applicable

Permission to reproduce material from other sources: Not applicable.

Abstract

Background: Neural crest cells (NCCs) are migratory embryonic stem cells that give rise to a diverse set of cell types and traits. Here we describe NCC migration and differentiation in the common wall lizard *Podarcis muralis* inferred from immunohistochemistry and *in situ* hybridization combining eleven markers.

Results: We find that oviposition occurs from about somite stage 13 (13ss), at which time migration of NCCs is well underway. In the stages investigated here, cranial NCC migration occurs in three main streams, one starting from the midbrain-hindbrain boundary and two in the caudal hindbrain separated by the otic vesicle. Migration in the trunk proceeds progressively more posteriorly as reported for other tetrapods. NCC differentiation towards mesenchymal fates is observed in craniofacial regions from 21ss, and differentiation towards neuronal fates occurs from 22ss.

Conclusions: We find that some markers show labelling patterns that are distinct from those described in other tetrapod species. However, the information emerging from all markers combined shows that the overall behavior of NCCs in the common wall lizard is largely conserved with that of other tetrapods. Our study highlights the dynamic nature of seemingly canonical marker genes and provides the first detailed spatiotemporal profiling of NCCs in a lacertid lizard.

Introduction

Neural crest cells (NCCs) are transient, migratory, stem cells that are unique to vertebrates and that give rise to many different cell types and thus contribute to a diversity of traits. NCCs are specified in the dorsal neural tube from where they delaminate in an epithelial-to-mesenchymal transition (EMT) and subsequently migrate throughout the embryo and differentiate. The cell types they give rise to include chromatophores responsible for skin color, osteocytes and chondrocytes that constitute the facial skeleton, neurons and glia of the peripheral nervous system and endocrinal chromaffin cells in the adrenal gland.[1]

NCCs originated at the dawn of vertebrates, and many of the vertebrate key innovations (most notably the jaw and other craniofacial structures) develop from NCCs.[2] For this reason, a substantial body of research has targeted the evolutionary origin of NCCs by investigating NCCs in early branching vertebrates and NCC-like cells in non-vertebrate chordates (e.g.[3–5]). In addition to these attempts to elucidate the evolutionary origin of NCCs in a macro-evolutionary context, much research has focused on investigating their function and development in a number of model organisms, most notably mouse (*Mus musculus*), chicken (*Gallus gallus*), African clawed frog (*Xenopus laevis*) and zebrafish (*Danio rerio*). Motivation for this research partially stems from the fact that failure of NCC functions cause neurocristopathies, a highly heterogeneous family of congenital diseases,[6] which makes them relevant from a medical perspective.

In squamate reptiles (lizards and snakes), NCC biology has been investigated in three species: the California kingsnake (*Lampropeltis getula californiae*[7]), the Egyptian cobra (*Naja haje haje*[8]) and the veiled chameleon (*Chamaeleo calyptratus*[9]). The reports on the two snake species mainly focus on the migration of NCCs in the trunk, while the report in chameleon provides

a comprehensive description of both cranial and trunk NCCs. Both snakes and chameleons have highly derived body plans including NCC-derived traits such as skull morphology.

In the chameleon, cranial NCC migration starts between the somite stage 4 and 6 (4ss and 6ss),[9] which is similar to mouse (5ss[10–12]), human (4ss[13]) and chicken (6ss[14(p66)]). In general, cranial NCC migration typically follows three main dorsolateral streams.[15] The NCCs in the anterior-most stream are specified in the caudal midbrain and the first three rhombomeres of the hindbrain and contribute cells to the rostrum, maxillary process and first pharyngeal arch.[15] The second stream is constituted by NCCs that are specified in rhombomeres three through five (anterior to the otic vesicle) and migrate to the second pharyngeal arch.[15] And lastly, the NCCs in the third stream are specified in rhombomeres five and six (posterior to the otic vesicle) and migrate to the third pharyngeal arch.[15] In the chameleon, however, Diaz et al.[9] identified a fourth stream of cranial NCCs starting posteriorly to the third stream and migrating to the fourth pharyngeal arch. An equivalent stream has also been described in alligator (*Alligator mississippiensis*) and ostrich (*Struthio camelus*).[16]

NCC migration in the trunk follows multiple, periodic streams starting in the dorsal neural tube. Viewed in cross-sections in a transverse plane, these streams typically follow two different routes.[17–19] An early wave of migrating cells follows a ventromedial route traversing between somites and through the anterior portion of somites and giving rise to, for example, peripheral nervous system and chromaffin tissue.[17–19] A later wave follows a dorsolateral route and gives rise to chromatophores.[17–19] While this pattern seems to be largely conserved across tetrapods,[7–9] it has been reported that some NCCs in the second wave follow a ventromedial rather than dorsolateral route in the California kingsnake.[7] The equivalent was not reported for chameleon or cobra.[8,9]

In between and partially overlapping with the cranial and trunk NCCs, there is a small subpopulation of NCCs called vagal NCCs.[15] Similar to trunk NCCs, vagal NCCs migrate along dorsolateral and ventromedial routes.[20] The dorsolateral migrating NCCs reach the pharyngeal arches and the heart where they give rise to facial skeleton and the heart smooth muscles, respectively.[20] Some vagal NCCs of both the dorsoventral and ventromedial streams reach the foregut which they then follow caudally to form the enteric nervous system.[20] Vagal NCCs have not been described in squamates.

While these efforts in squamates have increased our understanding of NCC specification, migration and differentiation across vertebrates, evolutionary changes in NCC behavior and potentially associated phenotypic changes are currently underexplored.[21] Since NCCs give rise to functionally diverse and ecologically relevant traits ranging from coloration (e.g., pigment cells) and morphology (e.g., skull and jaw bones) to physiology and behavior (e.g., adrenal gland influencing aggression), their coupling in a shared developmental origin can potentially have evolutionary consequences. Indeed, this coupling has been suggested to explain the domestication syndrome, which is based on the observation that domesticated animals share a set of changes in NCC-derived traits.[22,23] In general, due to their central role during development, modifications in the regulation of NCCs are expected to have the potential to generate biases in micro-evolutionary variation in natural populations of vertebrates and therefore contribute to adaptation and diversification.[21,24,25] To evaluate hypotheses like these, establishing patterns of NCC migration in species where NCCs may be implied in micro-evolutionary adaptation is crucial.

Here we present a description of NCCs in the common wall lizard (*Podarcis muralis*), which is a small (approx. 50–70 mm snout-to-vent length[26]), egg-laying lacertid. This species belongs to a genus of lizards distributed in the Mediterranean and Southern/Central Europe that

shows high variation in coloration and color patterns.[27,28] Within the common wall lizard, there is substantial variation in predominantly NCC-derived traits, namely coloration (ranging from brown/tan to black/green),[29–32] social behavior (in particular aggression in male-male interactions),[33,34] and morphology (e.g., body size, head size and shape).[29,32] In Italy, the strength of expression of these traits is tightly correlated across the landscape, culminating in the *nigriventris* syndrome at one end of the extreme and the ancestral phenotype at the other end.[32] The genetic basis of these trait differences has been identified as being polygenic, with more than half of all identified genes having a known association with the regulation of NCCs.[32] This prompted us to investigate NCC biology in this species. Females typically lay 2-3 clutches per breeding season with 2-10 eggs per clutch.[26(p189)] We used a set of eleven NCC markers that target different aspects of NCC biology to investigate the spatial distribution and inferred migration patterns of NCCs from the earliest stage at oviposition (~13ss) until the latest stages of NCC activity (~ 64ss). To identify evolutionary changes to NCC regulation, we compare our observations to equivalent patterns described in other squamates and more distantly related tetrapods. We find broad conservation in general NCC specification, migration, and differentiation, but also taxonomic differences in the expression patterns of individual markers. Taken together, our description of spatial and temporal patterns of NCCs during embryonic development expands our understanding of taxonomic diversity in NCC biology and presents a first step towards investigating the role of NCCs in shaping micro-evolutionary patterns.

Results and Discussion

Given that NCCs are a heterogeneous and highly dynamic cell population, there is no single marker that distinguishes them from all other cell types throughout development. We therefore use a two-

pronged approach to resolve spatiotemporal dynamics of putative NCCs. Firstly, we use immunostaining with antibodies against Human Natural Killer 1 (HNK-1) to label putative NCCs throughout development. HNK-1 is a carbohydrate on the cell surface of NCCs that is involved in cell-cell communication during migration[35,36] and it is a widely used marker of newly formed and migrating NCCs[16,17,37–43] (note however that it is not labelling NCCs in mouse)[44]. This antibody has been successfully applied to other squamate species,[7–9] which allows a straightforward comparison between our observations in the common wall lizard and other squamates.

Since HNK-1 is known to also label other cell types, in particular at late developmental stages,[45] we complemented HNK-1 immunostainings with gene expression analyses of NCC marker genes. For this second approach, we selected a panel of ten marker genes whose expression patterns were visualized using *in situ* hybridizations. Collectively, these marker genes label the majority of NCC subpopulations and target various stages of NCC development.[46] Note however that some markers do not exclusively label NCCs since they fulfil pleiotropic functions (e.g., *Twist1* stains mesodermal cells in addition to NCCs[47]). Specifically, we selected *Wnt1* and *Snai2* to label predominantly early NCCs, *Snai1*, *Twist1,* and *Sox9* to mark NCCs biased towards mesenchymal fates and *FoxD3*, *Sox10, Phox2b,* and *Eya2* to mark NCCs biased towards neuronal fates.[46,48,49] In addition, we used *Tyrosine hydroxylase* (*Th*) to label NCCs differentiating into chromaffin cells.[50] While HNK-1 immunostaining and *in situ* hybridizations provide snapshots of spatial and temporal patterns of NCCs in embryonic wall lizards, we infer migratory routes through extrapolations from the observed imaging data aided by comparisons to relevant literature.

HNK-1

HNK-1-positive cells are present in all investigated stages (five stages ranging from 13ss to 35ss) as shown by immunohistochemistry (Figure 1A-S). Cranial NCC migration is most pronounced in younger embryos while NCC migration in the trunk is induced at progressively more caudal levels with increasing embryonic age. Through all investigated stages, there is extensive HNK-1 signal in the heart (Figure 1A, M, Q, R and S). Strong staining in the heart was also reported in the chameleon.[9] However, the staining in the heart presumably does not exclusively mark cardiac NCCs since these are expected to have a more restricted distribution and to appear at later developmental stages.[51] Previous work in mammals, birds and reptiles found HNK1 to stain elements of the cardiac conduction system that are known to not develop from NCCs in the heart.[52–55]

Three streams of migratory cranial NCCs are inferred from the HNK-1 immunostaining. Each stream originates in the dorsal midline and extends ventrally in the developing head (Figure 1 A, E, F and M; dashed arrows outline inferred streams). The first stream starts at the level of the midbrain-hindbrain boundary and the two other streams begin more caudally in the hindbrain, one rostral and one caudal to the otic vesicle.

The first stream reaches towards the rostrum, maxillary process and the first pharyngeal arch (also known as the mandibular arch). Cross-sections through the head show that NCCs in this stream are migrating through the subectoderm (Figure 1C). The second inferred stream originates in the hindbrain just rostral to the otic vesicle extending towards the second pharyngeal arch (also known as the hyoid arch; Figure 1E and F). While the two first streams are visible already at the first investigated stage (13ss), the third stream appears around 17ss and starts just caudally to the otic vesicle and reaches towards the third pharyngeal arch (Figure 1E and F). In cross-sections through the second and third stream, dorsolateral migration can be inferred leaving the dorsal

neural tube and extending to the pharyngeal arches (Figure 1H and I). At this stage, the otic vesicle shows strong HNK-1 signal, which is maintained until the last investigated stage.

The three streams of migrating cranial NCCs remain recognizable until 22ss after which migration of cranial NCCs presumably seizes. By 22ss, HNK-1 signal is widely spread in the developing head including rostrum, maxillary process, and the first three pharyngeal arches (Figure 1M). There is also signal in the otic, olfactory and trigeminal nerve placodes (Figure 1M), which are co-derived from NCCs and placodal cells.[56,57] HNK-1 signal in the cranial peripheral nervous system is maintained as the cranial placodes give rise to cranial nerves (35ss), most notably the ophthalmic and maxillary branches of the trigeminal nerve and the ciliary ganglion (Figure 1S; cranial nerve nomenclature follows Diaz et al. (2019),[9] Lee et al. (2003)[57] and Streeter (1905)[58]).

At vagal levels, NCC migration can first be inferred along a dorsolateral route to the heart (Figure 1D). At later developmental stages, there is a weak signal extending caudally into the trunk from the third cranial stream, which potentially indicates a stream of vagal NCCs on their way to populate the gut (indicated with “Va” in Figure 1E). Cross-sections of the trunk reveal staining around the gut (Figure 1J-L), which most likely represents vagal NCCs of the developing enteric nervous system. Similar staining has been shown in chicken.[38]

In the trunk, HNK-1 signal in NCCs can be roughly divided into four stages: premigratory, early migratory, migratory, and early neural differentiation. HNK-1 signal is present in a stripe along the dorsal midline where premigratory NCCs are expected (Figure 1G and P). Immediately lateral to the dorsal midline, HNK-1 stains early migratory NCCs in loose cell aggregates, not yet forming migratory streams (asterisks in Figure 1A, B, E, G and N). The staining of these two stages

of NCCs is found at progressively more posterior positions along the trunk as development proceeds.

Following the expression in premigratory and early migratory NCCs, multiple streams of migrating NCCs can be inferred from HNK-1 staining. The inferred migratory streams are most notable between the somites (arrows in Figure 1A, B, E, G, N and P), but migration can also be inferred at the level of the somites (open arrow in Figure 1N). Cross-sections at different anterior-posterior positions along the trunk reveal that the streams of migratory NCCs take a ventral route between somites (inter-somitic; Figure 1J), while they take a dorsolateral route at the levels of the somites (Figure 1K). NCC migration in the most caudal region of the trunk is still ongoing in the oldest investigated stages (28ss and 35ss; Figure 1P).

Both dorsal and lateral views show a series of condensations of HNK-1 signal ventral to the somites along the trunk (arrowheads in Figures 1E and G). In cross-section, these locate approximately where we would expect to find sympathetic ganglia (arrows in Figure 1L). Later in development, roughly around 22ss, there is a diffuse field of weak HNK-1 staining along the trunk ventral to the somites (arrowhead in Figure 1N), presumably at the position of the developing sympathetic chain and the adrenal gland. In later stages, there is some HNK-1 staining in the mesonephros (arrows in Figure Q-S and S). This is also seen in other reptiles, but it is unclear if it is due to NCCs contributing to these structures.[7,9]

At later stages (35ss), we detect HNK-1 signal in the aorta and heart (Figure 1V). Presumably, this is caused by the fact that blood cells possess HNK-1 on their cell surface, despite not being NCC-derived.[45] Similarly, the segmental HNK-1 signal in the rhombomeres of the hindbrain (Figure 1R) is most likely stemming from non-NCCs in the central nervous system derived from the neural tube.

While HNK-1 signal is known to mark the NCC-derived dorsal root ganglia in chicken,[38] and also a turtle (*Trachemys scripta*)[59], an alligator (*Alligator mississippiensis*)[16] and the Californian kingsnake (*Lampropeltis getula calilforniae*),[7] this staining is absent in common wall lizards (Figure 1N and S). The reported HNK-1 staining in dorsal root ganglia in chameleon is also less distinct than in other organisms.[9] This emphasizes that HNK-1 is neither specific, nor general enough to figure as a sole NCC marker, and therefore requires complementation with other markers.

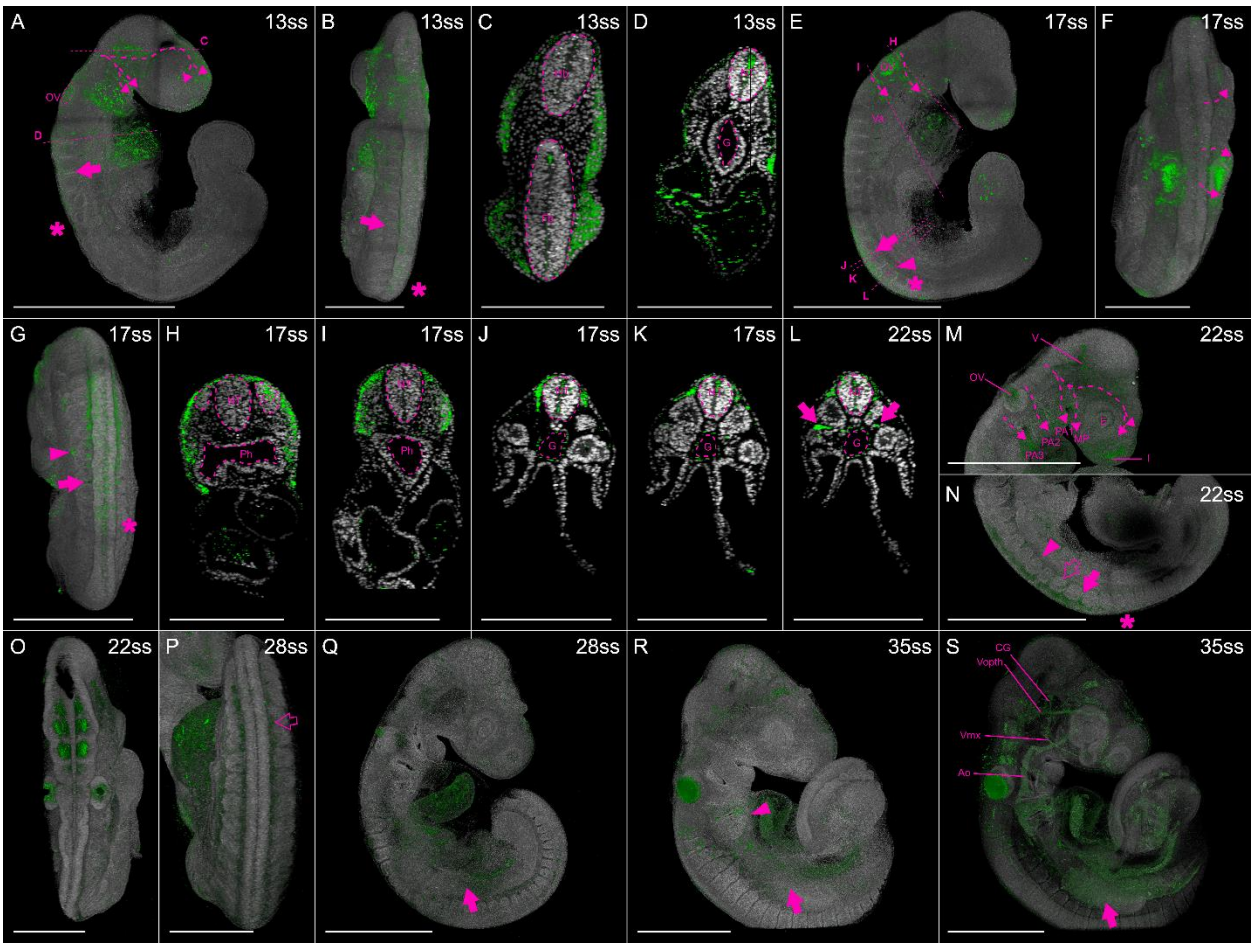

Figure 1. Immunohistochemistry of HNK-1 stains migratory and some early differentiating NCCs in common wall lizard embryos. A-D 13ss embryo in lateral (**A**) and dorsal (**B**) view, and in optical cross-sections (**C**, **D**). In **A**, dashed arrows indicate the first stream of inferred NCC migration and dashed straight lines indicate the approximate positions of the optical cross-sections at the level of the first inferred stream

of cranial NCCs (**C**) and at the level of the heart (**D**). Arrows in **A** and **B** indicate inter-somitic streams of trunk NCC migration and asterisks indicate early migratory NCCs that have not formed streams yet. **E-L** 17ss embryo in lateral (**E**), anterior dorsal (**F**), and posterior dorsal (**G**) view, and in optical cross-sections (**H-L**). In **E**, dashed straight lines indicate the approximate positions of the optical sections in panels **H-L** (level of the second (**H**) and third (**I**) inferred stream of cranial NCCs, and between (**J**) and within (**K**, **L**) somites). Dashed arrows indicate the second and third (**E**), and the first, second and third (**F**) streams of cranial NCC migration. In **E** and **G**, arrows indicate inter-somitic streams of trunk NCC migration, asterisks indicate early migratory NCCs, and arrowheads indicate a condensation of strong HNK-1 signal ventral to a somite. In **E**, weak signal of potential caudally migrating vagal NCCs are indicated with "Va". In **L**, arrows indicate strong signal in the presumed sympathetic ganglia. **M-O** 22ss embryo in lateral (**M**, **N**) and dorsal (**O**) view. In **M**, dashed arrows indicate the first, second and third inferred streams of cranial NCC migration. In **N**, arrow indicates an inferred inter-somitic stream of NCC migration, open arrow indicates migration at the level of a somite, asterisk indicates early migratory NCCs, and arrowhead indicates vague signal along the ventral side of the somites where the sympathetic chain is expected to develop. **P**, **Q** 28ss embryo in posterior dorsal (**P**) and lateral (**Q**) view. Open arrow indicates inter-somitic NCC migration and the filled arrow indicates signal in the mesonephros. **R**, **S** 35 embryo in lateral view rendered with different digital settings. Image in **S** was generated with low DAPI-opacity to emphasize the internal HNK-1 staining. In **R** and **S**, arrows indicate signal in the mesonephros. In **R**, arrowhead indicates signal in the fourth and fifth pharyngeal arches. In **S**, prominent cranial nerves are labeled. **Abbreviations:** E, eye; Fb, forebrain; G, gut; Hb, hindbrain; MP, maxillary process; NT neural tube; OV, otic vesicle; PA1-3, pharyngeal arch 1-3; Ph, pharynx; Va, vagal. **Cranial nerves:** I, olfactory nerve (also known as cranial nerve 1); V, trigeminal nerve (also known as cranial nerve 5); Vmx, maxillary branch of the trigeminal nerve; Vopth, ophthalmic branch of the trigeminal nerve. **Scale bars** in **B-D**, **F-L** and **O-P** are 0.5 mm, all other scale bars are 1 mm.

Gene expression profiles of early NCC marker genes (*Wnt1* and *Snai2*)

Besides being a crucial regulator of the midbrain-hindbrain region,[60] *Wnt1* is a classic marker of the neural border (including the rhombic lips[61]) and inducer of NCC specification,[46,62] and the *Wnt1-Cre* transgenic lines have been instrumental in numerous experimental studies in mice.[48,63,64]

Wnt1 is expressed in all investigated stages (10 stages ranging from 13ss to 60ss), mostly along the dorsal midline (Figure 2A-J). Through most of embryonic development (16-30ss), there is a noticeable gap of expression in the most anterior part of the hindbrain (the metencephalon; asterisks in Figure 2B and D-H) separating the expression into an anterior and a posterior domain. This pattern has been described in chicken.[60] The gap of expression overlaps with the origin of the first cranial stream as inferred from HNK-1 staining.

The anterior domain runs along the dorsal midline of the head from the level of the diencephalon (Figure 2B, C, F and G) to the midbrain-hindbrain boundary where it extends laterally in the direction of the eye on either side (arrowheads in Figure 2B and F). In the earliest investigated embryonic stages (13-16ss), the lateral expression at the level of the posterior midbrain is superficial. As development progresses, this expression pattern is internalized and forms a circle around the central nervous system by the midbrain-hindbrain boundary (Figure 2H-J). It also expands rostrally along the ventral midline of the midbrain (arrow in Figure 2G). By 16ss, there is also a lateral expansion of *Wnt1* expression in the rostrum (arrow in Figure 2B and C), which is not present in older embryos.

The posterior domain consists of two parallel lines running along the rhombic lips outlining each rhombomere in the hindbrain (Figure 2B, D-J) and continuing caudally along the dorsal midline of the trunk (Figure 2 D). In the trunk, *Wnt1* expression is evident along the dorsal midline extending approximately to the last formed somite pair (Figure 2B) and continuously extends posteriorly as development progresses (Figure 2F, G and J). The caudal extension of *Wnt1*

expression is concordant with premigratory NCCs as inferred from HNK-1 staining. While the signal along the midbrain-hindbrain boundary and the dorsal midline of the head remains strong throughout development, the signal in the trunk and hindbrain gradually fades in the oldest stages (51ss and onwards), although expression never fully disappears.

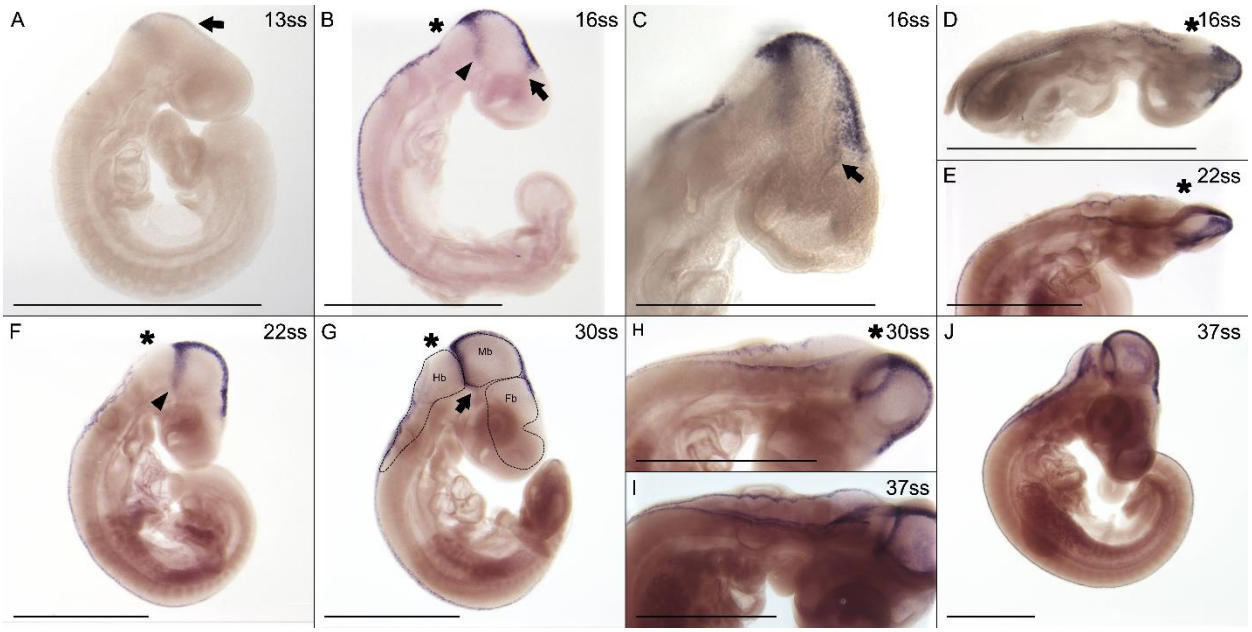

Figure 2. *Wnt1* is expressed along the dorsal midline. A 13ss embryo in lateral view. Arrow indicates expression along the dorsal midline of the midbrain. **B-D** 16ss embryo in lateral view (**B**), rostro-lateral view focusing on the head (**C**) and dorsolateral view (**D)**. In **B** and **C**, arrows indicate lateral expansion at the level of the forebrain. **E-F** 22ss embryos in dorsolateral (**E**) and lateral (**F**) view. In **B** and **D-H**, asterisks indicate a gap with no expression in the anterior hindbrain. In **B** and **F**, arrowheads indicate lateral expansions at the level of the midbrain-hindbrain boundary. **G, H** 30ss embryos in lateral (**G**) and dorsolateral (**H**) view. In **G**, arrow indicates expression on the ventral surface of the midbrain. Dashed lines in **G** indicate the outlines of the fore-, mid- and hindbrain. **I, J** 37ss embryos in dorso-lateral (**I**) and lateral (**J**) view. **Abbreviations:** Fb, forebrain; Hb, hindbrain; Mb, midbrain. **Scale bar** in **C** is 0.5 mm, all other scale bars are 1 mm.

Snai1 and *-2* are classical NCC markers previously known as *Snail* and *Slug*.[65] They are transcription factors that control cadherin-transcription and thereby EMT.[46] There was some uncertainty in regards to the homology relationships between these genes, and EMT is induced by paralogous genes in chicken (*Snai2*) and mouse (*Snai1*).[66] We confirmed the expected orthology relationships between *Snai1* and *-2* of the common wall lizard and their homologs in human, mouse and chicken (Supplementary figure 1) and investigated both of them using *in situ* hybridization. *Snai2* expression was investigated in eight stages ranging from 13ss to 51ss.

Snai2 expression in the head is found along the dorsal midline and the rhombic lips in the hindbrain (Figure 3A, C, D and G) and in the three streams of cranial NCC migration inferred with HNK-1 staining (dashed arrows in Figure 3B, D, E and G). In cross-section through the second inferred stream of cranial NCC migration, *Snai2* expression can be seen from the neural crest to the pharyngeal arches (Figure 3E). *Snai2* expression at this level is not restricted to the subectoderm.

The *Snai2* expression in the cranial streams is largely similar to that of HNK-1. However, while a caudally migrating vagal stream of NCCs is only weakly suggested by HNK-1 it is strongly marked by *Snai2* expression, visible as a branch from the third cranial stream turning caudally and entering the trunk (Figure 3D and G). In cross-section at the anterior-posterior-level of the heart (roughly at somite 4), strong *Snai2* expression is located lateral to the gut, presumably indicating caudally migrating vagal NCCs (Figure 3F).[20]

Compared to the HNK-1 staining, *Snai2* expression shows the three cranial streams as less separated from one another. The inference from *Snai2* alone would be that some cells from the second and third streams would converge to their respective anterior stream and contribute cells

to the pharyngeal arch typically populated by that stream. This scenario is not supported by HNK-1 staining, and has also not been described in lineage tracing studies in other organisms.[12,15] In older embryos, expression in the head is much reduced but there remains a low level of *Snai2* expression in the first three pharyngeal arches (arrowhead in Figure 3H), and weak expression in the caudal hindbrain.

Similar to HNK-1, *Snai2* expression in putative premigratory NCCs along the dorsal midline of the trunk progressively extends caudally as development progresses (arrows in Figure 3A, D, G and H). *Snai2* expression is also evident in multiple streams of migratory NCCs traversing the somites (Figure 3D and G, arrow in D). At later stages, the expression in the dorsal midline is only evident in the tail (arrow in Figure 3H), where it is accompanied by a ventral expression, which putatively represents migratory sacral NCCs.

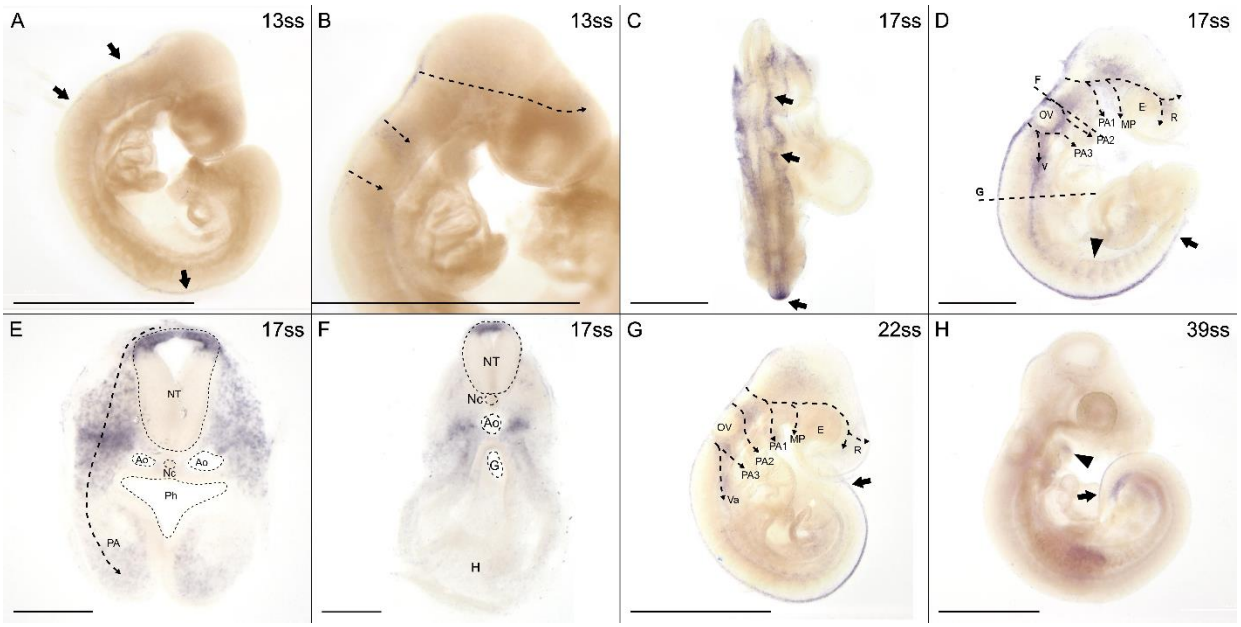

Figure 3. *Snai2* is expressed in both premigratory and migratory NCCs. A, B, whole (**A**) and head (**B**) of 13ss embryo in lateral view. Arrows indicate expression along the dorsal midline and dashed arrows highlight weak expression in the inferred streams of cranial NCC migration. **C-F** 17ss embryo in dorsal (**C**) and lateral (**D**) view and in cross-sections (**E, F**) at the levels indicated in **D**. Arrows indicate expression

along the dorsal midline and the rhombic lips an arrowhead indicates migration through the anterior half of the somites and dashed arrows indicate the inferred streams of migratory cranial NCCs. **G** 22ss embryo in lateral view. Dashed arrows indicate inferred streams of cranial NCC migration, and an arrow indicates expression along the dorsal midline. **H** 39ss embryos in lateral view. Arrow indicates expression in the dorsal midline and arrowhead indicates expression in the pharyngeal arches. **Abbreviations:** Ao, aorta; E, eye; G, gut; H, heart; MP, maxillary process; Nc, notochord; NT, neural tube; OV, otic vesicle; PA, pharyngeal arch; Ph, pharynx; R, rostrum; Va, vagal NCCs. **Scale** bar in **C** is 0.5 mm and scale bars in **E** and **F** are 0.1 mm. All other scale bars are 1 mm.

Taken together, *Wnt1* and *Snai2* confirm the spatiotemporal distribution of NCC induction and EMT. In addition, *Snai2*, but not *Wnt1*, is expressed in migratory NCCs, like HNK-1. *Snai2* is also expressed in putative vagal and sacral NCCs. As in chicken, but not mouse, *Snai2* seems to be expressed in NCCs undergoing EMT.[66]

Gene expression profiles of NCCs biased towards a mesenchymal fate (*Snai1, Twist1 and Sox9*)

Snai1 is expressed in all investigated stages (7 stages ranging from 16 to 51ss). In contrast to *Snai2*, *Snai1* is not expressed in the dorsal midline where premigratory NCCs are located. *Snai1* is therefore presumably not involved in EMT of NCCs in the common wall lizard, which is different from findings in mouse but consistent with findings in chicken.[66] However, its expression pattern in the head is concordant with that of migratory cranial NCCs and similar to the signals described for HNK-1 and *Snai2* above, especially in the first cranial stream (Figure 4A). In the trunk, most expression is located within somites and unsegmented caudal mesoderm, which is likely of non-NCC origin, and will therefore be disregarded in further description (Figure 4B).

Early expression (16-28ss) in the head is dominated by putative migratory NCCs. Later in development, *Snai1* expression is strongest in the maxillary process and pharyngeal arches (Figure 4C and D). These are structures in which NCCs are expected to settle and differentiate into chondrocytes and osteocytes that construct the facial skeleton. There is particularly strong expression in the maxillary process and the first pharyngeal arch, and from 44ss, *Snai1* expression is evident in the fourth and fifth brachial arches, though migratory streams are no longer visible (Figure 4D).

The different streams of cranial migration are not easily discernible for *Snai1* since the intensity of the expression signal is generally high. Given this high intensity, it is possible that not only NCCs contribute to the signal. At more posterior positions, *Snai1* expression indicates a stream of putative vagal NCCs (Figure 4A-C) that emerges from the third cranial stream, extends posteriorly, and bifurcates just caudally to the embryonic heart (arrow in Figure 4B).

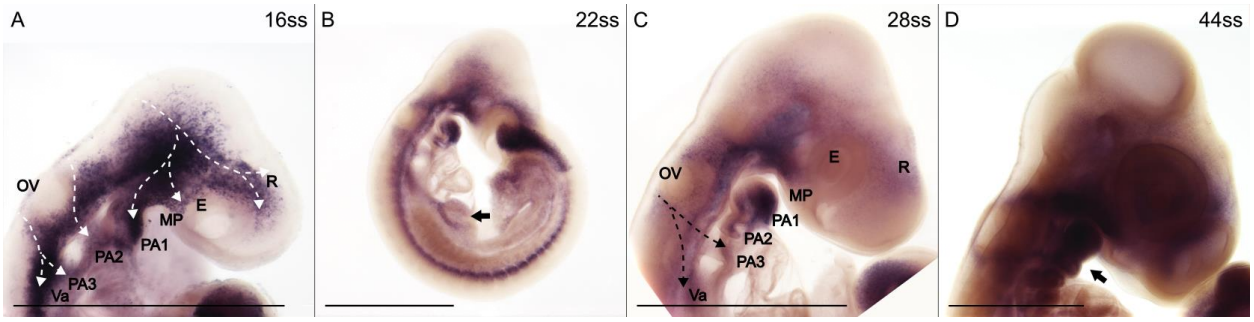

Figure 4. *Snai1* is expressed in migratory cranial NCCs. **A** Head of 16ss embryo in lateral view. Dashed lines indicate inferred streams of cranial NCC migration. **B** 22ss embryo in lateral view. Arrow indicates a bifurcation in the inferred caudal stream of vagal NCCs. **C** Head of 28ss embryo in lateral view. The dashed arrows indicate the third stream of inferred cranial NCC migration. **D** Head of 44ss embryos in lateral view. Arrow indicates strong expression in the pharyngeal arches. **Abbreviations:** E, eye; MP, maxillary process;

OV, otic vesicle; PA1-3, pharyngeal arch 1-3; R, rostrum; Va, posterior stream of vagal NCCs. **Scale bars** are 1 mm.

Twist1 is a well-known NCC marker and transcription factor which has been studied in various other organisms where it has been found to be involved in EMT,[67] maintenance of migratory phenotype, repression of neuronal differentiation,[68] and induction of chondrocyte differentiation.[48] Similar to *Snai1*, *Twist1* expression in the common wall lizard is missing in the dorsal midline but is consistent with the expected location of migratory cranial NCCs (dashed arrows in Figure 5A and B). The lack of *Twist1* expression in the presumed premigratory NCCs in the dorsal midline is consistent with findings in mouse and chicken,[68,69] but different from frog and zebrafish.[67]

Cranial expression of *Twist1* is observed in all investigated stages (7 stages ranging from 13 through 51ss; Figure 5A-H) with a gradual change in the overall expression pattern occurring around 28-35ss. Prior to that, *Twist1* is mainly expressed in the putative streams of migratory cranial NCCs (Figure 5A-D, dashed arrows in A, C and D), but after this point, expression is mostly restricted to the maxillary process and pharyngeal arches (arrow and arrowhead in Figure 5F). Given the described role of *Twist1* as an inducer of chondrocytes,[43] this gene is likely crucial for the formation of craniofacial structures in this region. At these early stages, there is also broad but transient expression of *Twist1* in the head ectoderm. Later in development, there is strong *Twist1* expression in a circle around the olfactory pit (arrow in Figure 5G-H).

Similar to *Snai1* and *Snai2*, *Twist1* is also expressed in a stream of putative vagal NCCs branching from the third cranial stream posterior to the otic vesicle (Figure 5D). While *Twist1* is extensively expressed in the trunk, it is mostly restricted to putative mesodermal cells in the somites and limb buds and will therefore be disregarded here.

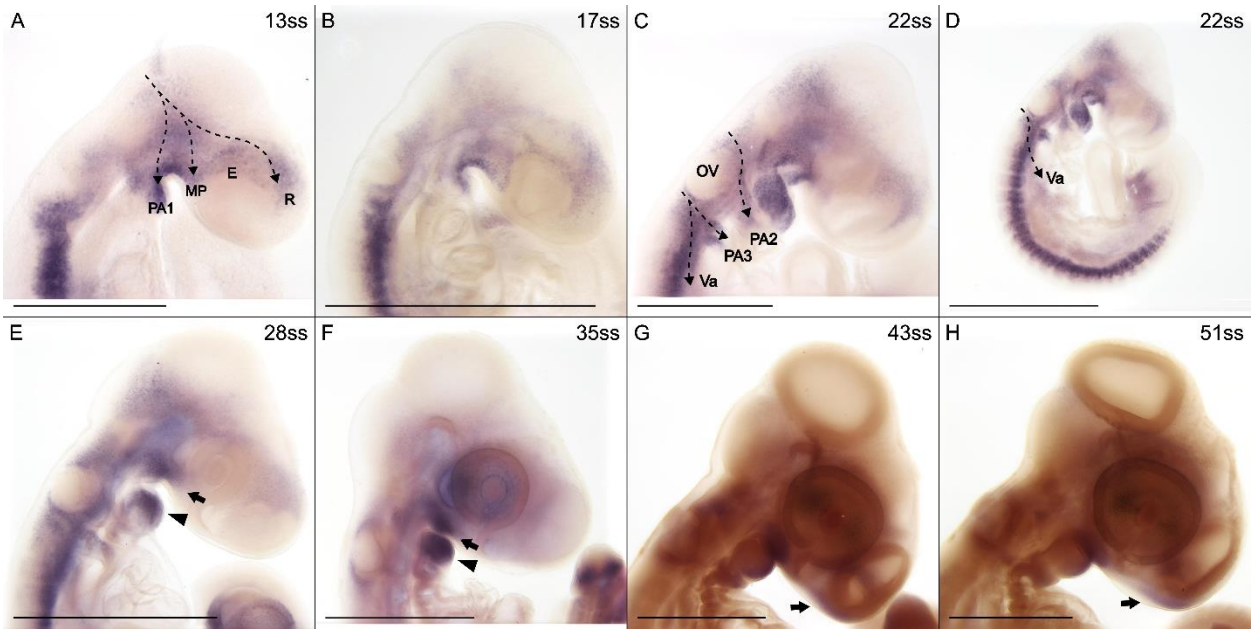

Figure 5. *Twist1* is expressed in migratory cranial NCCs. **A-C** Heads of 13, 17 and 22ss embryos in lateral view. Dashed lines indicate the inferred streams of cranial NCC migration. **D** 22ss embryo in lateral view. The dashed arrow indicates an inferred caudal stream of vagal NCC migration. **E-F** Head of 28 and 35ss embryos in lateral view. Arrows indicate the maxillary process and arrowheads indicate the first pharyngeal arch. **G-H** Head of 43 and 51ss embryo in lateral view. Arrow indicates olfactory pit. **Abbreviations:** E, eye; MP, maxillary process; OV, otic vesicle; PA1-3, pharyngeal arch 1-3; R, rostrum; Va, posterior stream of vagal NCCs. **Scale bar** in **A** is 0.5 mm, all others are 1 mm.

Together with *Snai1* and *-2*, *Sox9* is known to be a crucial regulator of EMT,[46,70] and it is also known to regulate migration and chondrocyte differentiation of cranial NCCs.[46] However, in the trunk, *Sox9* is expressed in premigratory but not migratory NCCs.[71] In the common wall lizard, *Sox9* is expressed in all investigated stages (8 stages ranging from 13ss through 51ss; Figure 5A-D).

In the common wall lizard, *Sox9* appears to label both premigratory and migratory NCCs in the head. At 17ss, there is strong expression in the dorsal midline by the fore- and midbrain and along the rhombic lips of the hindbrain (Figure 6A and B). In addition, elements of the three cranial

streams inferred from HNK-1 staining are also evident from *Sox9* expression (dashed arrows in Figure 6A). In the third stream, it is mainly the caudally directed putative vagal branch that can be inferred (Figure 6A and B).

Later in development, the expression in the inferred streams extends to much of the surface of the head. By 22ss the streams can still be distinguished but are somewhat obscured by the widespread expression (Figure 6C), and by 28ss the streams can no longer be distinguished (Figure 6D). Expression is especially strong in the first pharyngeal arch, maxillary process, ventral to the eye, by the nasal placode, in the rostrum and by the forebrain-midbrain border (Figure 6C).

Sox9 expression in the trunk is consistent with premigratory NCCs along the dorsal midline but not with migratory NCCs. There is also expression in non-NCC related structures such as limb buds, somites and migratory mesodermal cells delaminating from the somites (Figures 6A and C), which will not be described in more detail here. This is consistent with findings in chicken.[71] Some *Sox9* expression can be seen in the heart. This is most noticeable at 39ss (Figure 5D) where it stains a structure that may be the outflow tract, which is partially derived from NCCs.[68]

The posterior extent of the expression along the dorsal midline extends slightly further than the last formed somite pair, progressively extending caudally throughout development (asterisks in Figure 6A, C and D). There is also expression in what appear to be early migratory NCCs just lateral to the dorsal midline that have not jet condensed into migratory streams (Figure 6A-C). In older stages, the more anterior expression in the dorsal midline fades and by 39ss it only remains detectable in the tail (asterisk in Figure 6D).

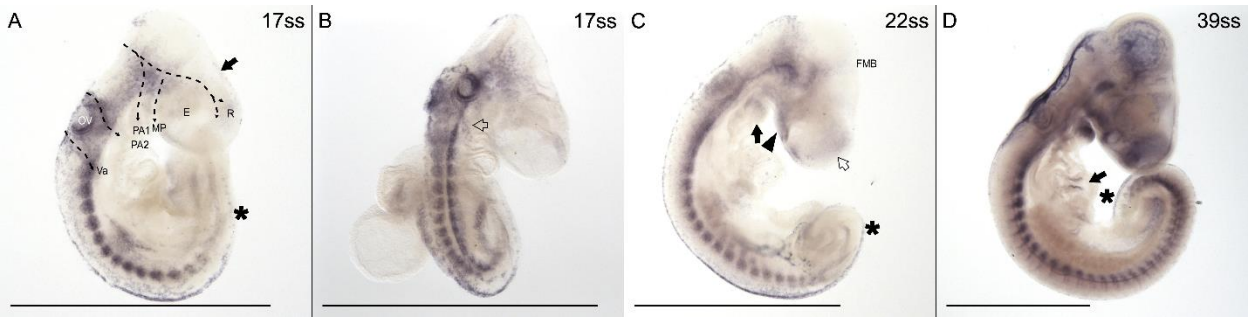

Figure 6. *Sox9* expression labels both premigratory NCCs and migratory cranial NCCs. A, B 17ss embryo in lateral (**A**) and dorsolateral (**B**) view. Dashed lines indicate inferred streams of cranial NCC migration. Asterisk indicates caudal extent of expression along the dorsal midline, arrow indicates expression in the dorsal midline at the level of the forebrain and open arrow indicates caudally directed putative migratory stream of vagal NCCs. **C** 22ss embryo in lateral view. Arrow indicates expression in the first pharyngeal arch, arrowhead indicates expression in the maxillary process, open arrow indicates expression in the rostrum and asterisk indicates expression along the dorsal midline of the tail. **D** 39ss embryo in lateral view. Asterisk indicates caudal extent of expression along the dorsal midline and arrow indicates expression in the heart. **Abbreviations:** E, eye; MP, maxillary process; OV, otic vesicle; PA, pharyngeal arch; R, rostrum; Va, posterior stream of vagal NCCs. Scale bars in **A**, **E** and **G** are 0.5 mm, all others are 1 mm.

The expression patterns of *Snai1*, *Twist1* and *Sox9* generally support the spatiotemporal location of migratory cranial neural crest cells inferred from HNK-1. In addition, they distinctly label regions such as the maxillary process and pharyngeal arches where facial skeleton will develop. *Sox9* is also expressed in the heart and in putative premigratory NCCs along the dorsal midline of both head and trunk.

Gene expression profiles of NCCs biased towards a neuronal fate (*FoxD3, Sox10, Eya2* and *Phox2b*)

FoxD3 is known to be an important transcription factor in NCC development.[17] Early in NCC development, *FoxD3* acts as an activator, allowing NCCs to delaminate from the neural tube, but later its role changes and it maintains the multipotency of NCCs by repressing differentiation.[18,72,73]

Similar to the HNK-1 staining, expression of *FoxD3* is found in both the putative premigratory NCCs along the dorsal midline and in the inferred streams of migratory NCCs in both head and trunk (Figure 7A-G). The expression in migratory NCCs in the trunk (Figure 7C, E and F) sets it apart from *Snai2* and *Sox9* (see above). *FoxD3* is also expressed in NCC-derived peripheral nervous system in both head and trunk (Figure 7E-H). It is expressed in all investigated stages (nine stages from 13 to 64ss).

In contrast to HNK-1 and the markers for mesenchymal-biased NCCs (*Snai1*, *Twist1* and *Sox9*), *FoxD3* expression does not stain the entire length of the inferred cranial streams. *FoxD3* expression does not extend to the pharyngeal arches, maxillary process, or the rostrum (Figure 7A and C). This reflects how NCCs with strong *FoxD3* expression are biased towards neuronal and glial fates, while NCCs with strong *Twist1* expression, for example, are biased towards mesenchymal fates. However, a stream of putative vagal NCCs extends caudally into the trunk (arrowheads in Figure 7E and F).

The neuronal bias of *FoxD3* expressing NCCs is also reflected in the gradual condensation of expression in the developing cranial peripheral nervous system. This is most prominent in the trigeminal (arrows in Figure 7E and F) and geniculate (open arrows in figure 7G and H) nerve placodes and subsequently in the corresponding cranial nerves (Figure 7G and H). Other elements of the developing cranial peripheral nervous system (such as the ciliary ganglion) are also expressing *FoxD3*.

FoxD3 expression in the trunk starts along the dorsal midline in presumed premigratory NCCs (asterisks in Figure 7A-G). This expression domain extends caudally as development progresses. At positions anterior to the premigratory NCCs, periodic streams of migratory NCCs traverse through each somite (Figure 7E). At later stages, these streams condense into the dorsal root ganglia (arrowhead in figure 7H) and the sympathetic chain ganglia (Figure 7G and H).

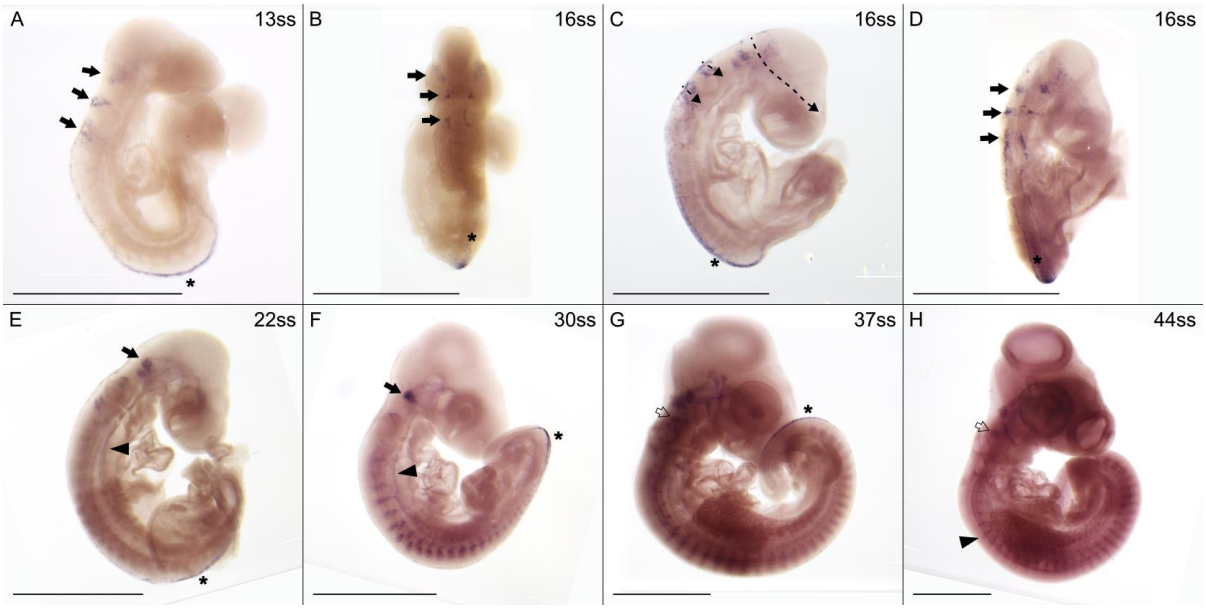

Figure 7. *FoxD3* expression labels both premigratory and migratory NCCs as well as developing peripheral nervous system. A, B 13ss embryo in lateral (**A**) and dorsal (**B**) view. Arrows indicate the first three inferred streams of migratory cranial NCCs. In **A-G**, asterisks indicate expression in premigratory NCCs along the dorsal midline. **C, D** 16ss embryo in lateral (**C**) and dorsal (**D**) view. Dashed arrows indicate three inferred streams of cranial NCC migration. Arrows indicate where these streams start. **E, F** 22 (**E**) and 30ss (**F**) embryos in lateral view. Arrows indicate the trigeminal nerve placode and arrowheads indicate a putative stream of vagal NCC migration. **G, H** 37 (**G**) and 44ss (**H**) embryos in lateral view. Open arrows indicate the geniculate ganglion (also known as cranial nerve ganglion 7). **Scale bars** are 1 mm.

After HNK-1, *Sox10* is arguably the most canonical NCC marker, and together with *FoxD3* and *Ets1* it is considered a NCC specifier gene.[46] It is a marker of migratory NCCs,[74] and it is necessary for NCC differentiation into melanocytes and neuronal fates.[46]

In the common wall lizard, *Sox10*, like *FoxD3*, is expressed in the migratory NCCs of both head and trunk, and in the developing peripheral nervous system. Unlike *FoxD3*, *Sox10* expression in the putative premigratory NCCs along the dorsal midline is weak. *Sox10* is expressed in all investigated stages (11 stages ranging from 13 to 64ss; Figure 8A-P).

All three streams of migratory cranial NCC inferred from the HNK-1 staining are clearly expressing *Sox10* (Figure 8A and B). However, *Sox10* expression, like *FoxD3*, does not extend ventrally to the pharyngeal arches or the rostrum. As development progresses, cranial *Sox10* expression localizes around some cranial placodes such as the otic vesicle (arrow in Figure 8G) and the trigeminal nerve placode (arrows in Figure 8H and I), both co-derived from NCCs and placodal cells.[56,57] At later stages, *Sox10* marks cranial nerves that are part of the cranial peripheral nervous system (Figure 8L, M and P; cranial nerve nomenclature follows Diaz et al. (2019)[9], Lee et al. (2003)[57] and Streeter (1905)[58]).

A putative vagal stream migrating caudally in the trunk from the third cranial stream is marked by *Sox10* expression (arrowhead in Figure 8H and K). Later in development, the vagus nerve is clearly distinguishable through *Sox10* expression (Figure 8P).

Sox10 expression in the trunk is largely similar to the spatiotemporal distribution of NCCs inferred from HNK-1 staining, although the expression in the putative premigratory NCCs along the dorsal midline is rather weak. As in HNK-1, early *Sox10* expression is found at anterior levels and late in development it is found in posterior levels (asterisks in Figure 8C, H, K and L). It is

dominated first by the serial streams of migratory NCCs, which were also inferred from HNK-1 staining (arrow in Figure 8C) and later by the developing peripheral nervous system (Figure 8L and O).

The migratory streams traversing the somites are rather broad but largely confined to the anterior part of the somites, each stream narrowing ventrally (Figure 8H and K). In cross-section at the level of the heart at 13ss, the inferred streams are revealed to migrate ventrally along the edge of the neural tube (Figure 8D-F). By looking at different levels along the anterior-posterior axis, two different routes of migration can be distinguished; one turns laterally and enters the somite about 1/10th from the ventral edge of the neural tube (Figure 8D and E). These will likely give rise to dorsal root ganglia.[18] The other one continues ventrally (Figure 8D and F) and will likely give rise to sympathetic ganglia.[18] Some migration seems to be ongoing in the tail even at 37ss (asterisk in Figure 8L).

The expression in the migratory streams subsequently condenses to a row of dorsal root ganglia in each somite with ventral projections to the much smaller ganglia of the sympathetic chain (Figure 8L). The dorsal root ganglia, including their dorsal and ventral roots, are clearly visible in cross-section, while sympathetic ganglia are evident more ventrally, though less strongly expressing *Sox10* (Figure 8O).

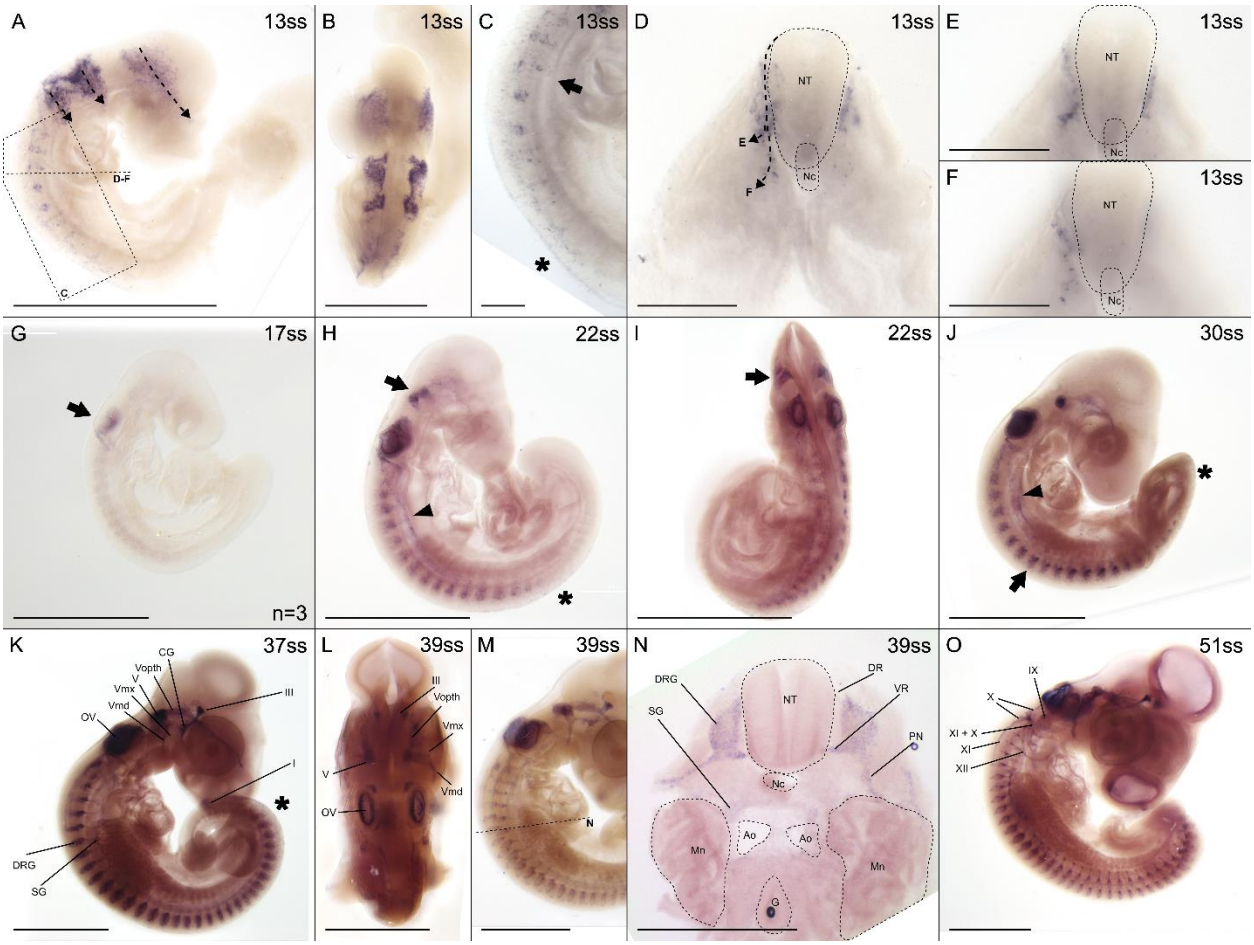

Figure 8. *Sox10* expression identifies migratory NCCs and the developing peripheral nervous system. **A-C** 13ss embryo in lateral (**A, C**) and dorsal (**B**) view. The dashed rectangle in **A** indicates magnified region shown in **C.** Dashed arrows indicate the inferred streams of cranial NCC migration, asterisk indicates weak expression along the dorsal midline and arrow indicates migratory streams in the trunk. **D-F** cross-section through the trunk at the level indicated in **A. D** is a composite of many focal planes, while (**E** and **F**) are different single focal planes. The dashed arrows indicate inferred streams of NCC migration. **G** 17ss embryo in lateral view. Arrow indicates the otic vesicle. **H, I** 22ss embryo in lateral (**H**) and dorsal (**I**) view. Asterisk indicates weak expression in premigratory NCCs along the dorsal midline, arrows indicate the trigeminal nerve placode and arrowhead indicates a putative stream of caudally migrating vagal NCCs. **J** 30ss embryo in lateral view. Asterisk indicates weak expression in the dorsal midline, arrow indicates putative streams of NCC migration in the trunk, gradually condensing into dorsal root ganglia, and

arrowhead indicates a putative stream of migratory vagal NCCs. **K** 37ss embryo in lateral view. Asterisk indicates weak expression along the dorsal midline. Several components of the peripheral nervous system are indicated in **K**, **L**, **N** and **O**. **L-N** 39ss embryo in dorsal (**M**) and lateral (**N**) view, and in cross-section (**N**). The approximate level of the cross-section in **N** is indicated by a dashed line in **M. O** 51ss embryo in lateral view. **Abbreviations:** Ao, aorta; CG, ciliary ganglion; DR, dorsal root; DRG, dorsal root ganglion; G, gut; Mn, mesonephros; Nc, notochord; NT, neural tube; OV, otic vesicle; PN, peripheral nerve; SG, sympathetic ganglion; VR, ventral root. **Cranial nerves:** I, olfactory nerve (also known as cranial nerve 1); III, oculomotor nerve (also known as cranial nerve 3); V, trigeminal nerve (also known as cranial nerve 5); Vopth, ophthalmic branch of the trigeminal nerve; Vmd, mandibular branch of the trigeminal nerve; Vmx, maxillary branch of the trigeminal nerve; IX, glossopharyngeal nerve (also known as cranial nerve 9); X, vagus nerve (also known as cranial nerve 10); XI, spinal accessory nerve (also known as cranial nerve 11); XII, hypoglossal nerve (also known as cranial nerve 12). **Scale bars** in **B** and **O** are 0.5 mm and **C**, **D**, **E** and **F** are 0.1 mm. All other scale bars are 1 mm.

Unlike *FoxD3* and *Sox10*, *Eya2* is not a typical NCC marker. However, *Eya1* and *-2* are known regulators of neurogenic placodes,[46] and Zang et al. (2021)[75] found that *Eya2* expression in a subset of cranial ganglia is exclusively stemming from NCC-derived cells.

Eya2 is expressed in both the head and the trunk in all the investigated stages (7 stages ranging from 17 to 51ss; Figure 9A-D). As in chicken (GEISHA[76]), and mouse,[75,77] *Eya2* expression in the head mostly localizes to the ectoderm of the pharyngeal arches (arrows in Figure 9B and D). The association to eyes, cranial placodes and ganglia in mouse and chicken is less evident in common wall lizards. However, weak expression occurs in the trigeminal nerve placode (arrow in Figure 9A), nasal placode (arrows in Figure 9C and D) and otic vesicle (asterisk in Figure 9D).

In the trunk, *Eya2* is expressed in the somites (asterisks in Figure 9B) already from the earliest investigated stage (17ss) and remains pronounced until 39ss. A similar pattern in mouse was interpreted by Zang et al. (2021) as developing dorsal root ganglia.[75]

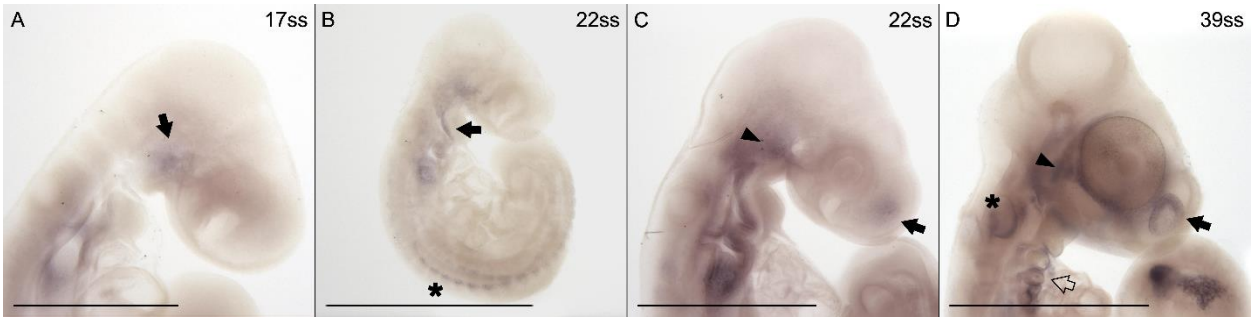

Figure 9. *Eya2* is expressed in the ectoderm of the pharyngeal arches. A Head of 17ss embryo in lateral view. Arrow indicates expression in the trigeminal nerve placode. **B** 22ss embryo in lateral view. Asterisk indicates expression in the somites, and arrow indicates expression in the pharyngeal arches. **C, D** heads of 22 (**C**) and 39ss (**D**) embryos in lateral view. Arrowheads indicate expression in the trigeminal nerve placode (**C**, 22ss) and trigeminal nerve (**D**, 39ss), arrows indicate expression in the nasal placode (**C**, 22ss) and around the olfactory pit (**D**, 39ss), asterisk indicates expression in the otic vesicle and open arrow indicate expression in the pharyngeal arches. Note that **B** and **C** do not show the same embryo. **Scale bars** in **A** and **C** are 0.5 mm the other scale bars are 1 mm.

Downstream of *Sox10, Phox2b* is a regulator of NCC differentiation into autonomic and especially sympathetic neurons and chromaffin cell progenitors.[46,78–80] In the common wall lizard, *Phox2b* is expressed in all investigated stages (7 stages ranging from 17-51ss) except the youngest (17ss; data not shown). However, the expression is most distinct at 39ss (Figure 10A-D), and expression before and after this stage is generally weak (Figure 10G). At 22ss, *Phox2b* is expressed at the level of the anterior hindbrain as a faint line internal to the embryo (Figure 10A. This expression domain continuously expands caudally as development progresses (arrows in Figure 10B).

At 39ss, *Phox2b* expression also localizes to several of the cranial ganglia (indicated in Figure 10B-D), which are co-derived from the cranial placodes and NCCs.[81] At this stage, there is also significant expression in the hindbrain in the form of three stripes on each side. In dorsolateral view one can distinguish a ventral stripe (arrow in Figure 10D), a medial stripe (open arrow in Figure 10D), and a dorsal stripe (arrowhead in Figure 10D), which is consistent with results in mouse.[82] Expression in the dorsal stripe (asterisk in Figure 10F) and the geniculate ganglion is also seen at 51ss.

In the trunk, *Phox2b* is expressed at 39ss in a longitudinal internal stripe matching the position of the sympathetic chain previously described in mouse (arrowheads in Figure 10A).[82] *Phox2b* is also expressed in a ventral domain caudal to the hindlimb buds (open arrow in Figure 10A). A similar domain was found with *Snai2* at the same developmental stage (Figure 3J) and may indicate migratory sacral NCCs. Contrary to previous results in mouse and chicken,[81,82] there was no distinct expression of *Phox2b* in the dorsal root ganglia in any of the investigated stages.

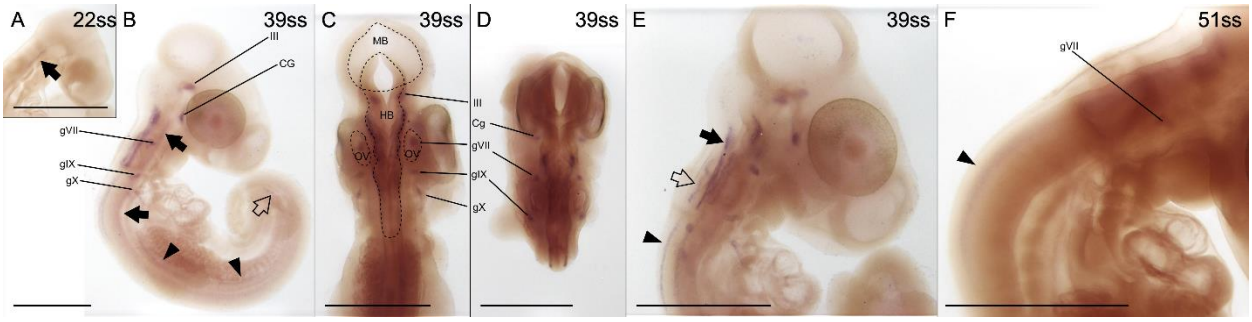

Figure 10. *Phox2b* expression identifies cranial ganglia and the developing sympathetic chain. A Head of 22ss embryo in lateral view. **B-D** 39ss embryo in lateral (**B**) and dorsal (**C**, **D**) view. Expression signals in several cranial nerve ganglia are indicated. In **A** and **B**, arrows indicate the faint internal line of expression, arrowheads indicate expression in the developing sympathetic chain, and open arrow indicates ventral expression in the tail. **E** Head of 39ss embryo in dorsolateral view. Arrows (open and filled) and arrowhead indicate expression in lateral lines in the hindbrain (see main text for more information). **F**

Hindbrain and anterior trunk of a 51ss embryo in lateral view. **Abbreviations of cranial nerves and ganglia:** CG, ciliary ganglion; III, oculomotor nerve (also known as cranial nerve 3); gVII, geniculate ganglion (also known as cranial nerve ganglion 7); IX, glossopharyngeal ganglion (also known as cranial nerve 9); X, vagus nerve (also known as cranial nerve 10). **Scale bars** are 1 mm.

Taken together, gene expression profiles of NCCs biased towards neuronal fates (*FoxD3* and *Sox10*, *Eya2* and *Phox2b*) largely confirm and expand the spatiotemporal distribution of NCCs inferred from HNK-1 staining. The contribution of NCCs to the development of the peripheral nervous system, including the sympathetic nervous system, is clearly visualized by the expression patterns of *Sox10*, *FoxD3*, and *Phox2b*.

Gene expression profiles of NCCs differentiating into chromaffin cells (*Th*)

A subset of the *Phox2b* positive cells in the trunk will develop into the chromaffin cells of the adrenal gland. In mouse, *Tyrosine hydroxylase* (*Th*) has been identified as a suitable marker for separating the chromaffin cells from the sympathetic neurons.[79,83]

Th expression is first detected at 35ss and is maintained at least until 51ss. The expression is located internally in the trunk, at the level of the forelimb bud (Figure 11A-F). *Th* expression is localized in two laterally parallel lines (Figure 11B) in the dorsomedial corner of the mesonephros (Figure 11D). This is putatively the position where the sympathetic ganglia including the adrenal glands are developing. The areas of expression are discontinuous (see for example arrowheads in Figure 11E) concordant with chromaffin cells being restricted to the sympathetic ganglia including the adrenal glands.

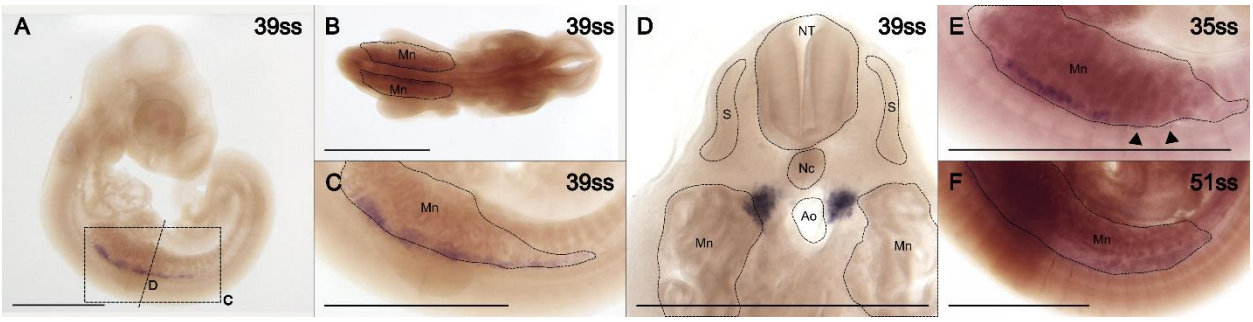

Figure 11. *Th* expression identifies the chromaffin cells of the putative adrenal gland. A-C 39ss embryo in lateral (**A, C**) and dorsal (**B**) view and in cross-section (**D**). Dashed rectangle and line in A indicate the approximate position of panels C and D respectively. **E, F** Trunk of 35 and 51ss embryos in lateral view. Arrowheads indicate discontinuity in the expression. **Abbreviations:** Ao, aorta; Mn, mesonephros; Nc, notochord; NT, neural tube; S, somite. **Scale bar** in **D** is 0.5 mm, all others are 1 mm.

An attempt to obtain expression patterns for *Mitf*, a marker gene of NCCs differentiating into pigment cells, remained unsuccessful and did not generate reliable expression patterns (see Supplementary Fig. 2).

Conclusions

Taken together, the insights gained from HNK-1 immunostainings and gene expression patterns of ten marker genes provides a detailed profile of the spatiotemporal distribution of NCCs in developing wall lizard embryos (Figure 12). By the time of egg-laying, the embryo has already reached at least 13ss at which extensive migration is ongoing in the head. Around 35ss, most migration is completed and differentiation towards various fates is well underway. In the following, we briefly summarize the major patterns of NCC development at four different stages.

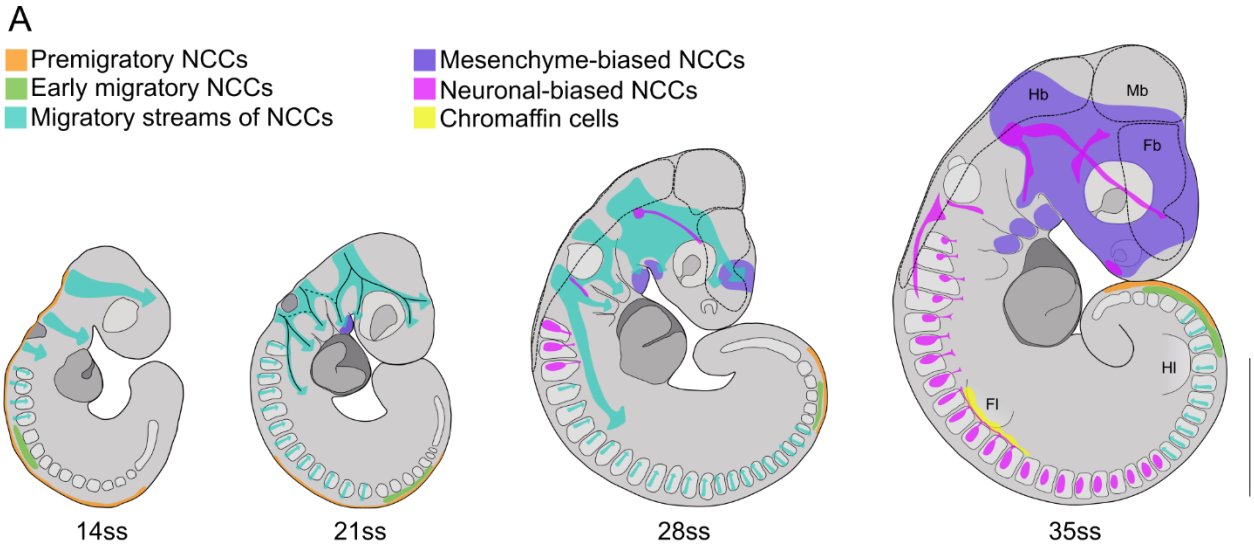

B

	Premigratory			Migratory			Differentiating		
	Cranial	Vagal	Trunk	Cranial	Vagal	Trunk	Cranial	Vagal	Trunk
HNK1									
Wnt1									
Snai2									
Snai1									
Twist1									
Sox9									
FoxD3									
Sox10									
Phox2b									
Eya2									
Th									

Figure 12. Synthesis of the spatiotemporal distribution of NCCs in developing common wall lizards. **A** Summary of the inferred distribution and migratory streams of NCCs in four developmental stages of the common wall lizards. Different groups of NCCs are color-coded according to their state or expected fate. **B** Schematic overview of the state of NCCs (premigratory, migratory or differentiating) and their respective domain (cranial, vagal or trunk) with respect to their expression of individual marker genes and the presence of HNK-1 positive staining. **Abbreviations**: Fb, forebrain; Fl, forelimb; Hb, hindbrain; Hl, hindlimb; Mb, midbrain.

At 14ss, premigratory NCCs are present along the dorsal neural tube all the way from the midbrain-hindbrain boundary to the last formed somite pair (orange in Figure 12A). Streams of cranial NCCs are already migratory, but their migratory routes have not started to bifurcate. In the caudal trunk, there is no migration observed at this stage. At more anterior regions in the trunk, a field of NCCs lateral to the dorsal midline indicates that the first wave of NCC migration has started but these cells have not yet entered the somites (green in Figure 12A). In the anterior-most part of the trunk, migration has proceeded further with the first migratory streams traversing the anterior parts of the anterior-most somites (turquoise in Figure 12A).

At 21ss, NCC specification and migration in the trunk has proceeded further posteriorly and migration now occurs through several of the anterior-most somites (approximately the first 13-15). In the head, the streams of migratory cranial NCCs have started to bifurcate and cells with mesenchymal fate are located in the first pharyngeal arch (purple in Figure 12A). Vagal NCCs appear as a stream extending caudally through the anterior trunk from the hindbrain.

By 28ss, NCC specification and migration in the trunk has proceeded even further posteriorly and the first differentiated dorsal root ganglia occur in the anterior-most somites (approximately the first 23; magenta in Figure 12A). The cranial streams are now more advanced and cells with mesenchymal fate appear in the maxillary process and the rostrum. Some differentiation towards cranial nerves has begun (magenta in Figure 12A).

At 35ss, specification and migration of NCCs is restricted to the posterior-most trunk region. Neuronal differentiation is well underway in both the dorsal root ganglia and the sympathetic ganglia of the trunk. At the level of the forelimb, some NCCs have differentiated into chromaffin cells (yellow in Figure 12A). The mesenchymal NCCs are now distributed broadly in the head including the first three pharyngeal arches, maxillary process, rostrum and close to the

olfactory pit. Cranial nerves have developed further, the olfactory (I), oculomotor (III), trigeminal (V), glossopharyngeal (IX), vagus (X) and spinal accessory nerves are now all clearly distinguishable.

This synthesis is derived from the collective information gathered from eleven markers (Figure 12B), which proved to be crucial to overcome incomplete information stemming from individual markers. For example, HNK-1 immunostaining and *Phox2b* expression signals are not located in the dorsal root ganglia, yet other markers, for example *Sox10* and *FoxD3*, clearly identify this tissue as NCC-derived. The HNK-1 signal in dorsal root ganglia reported for the veiled chameleon[9] is also less distinct than typically seen in other organisms, which may therefore be more widespread in lizards. In addition, since there are no distinct NCC markers that identify exclusively NCCs, off-target staining necessarily needs to be taken into account. Examples include the expression of *Snai1* and *Twist1* in trunk mesoderm or the presence of HNK-1 on blood cells.

Comparing our synthesis of NCCs in the common wall lizard to those reported for other squamates (the Californian kingsnake[7], Egyptian cobra[84] and veiled chameleon[9]) reveals that NCC biology is largely conserved. One caveat for this comparison is that our analysis is restricted to embryos older than 13ss, and we therefore lack observations of the earliest stages of NCC specification and migration, particularly in the head. It was therefore not possible to investigate if common wall lizards, similar to chameleons[9] and crocodiles[76], possess an early rostral stream of migrating cranial NCCs stemming from the level of the forebrain. In future studies, efforts could be made to obtain earlier embryos by, for example, treating gravid females hormonally to induce premature egg laying,[86] or by selecting lizard species that lay eggs at earlier developmental stages.

The two main exceptions of NCC regulation in squamates relative to other tetrapods that have been reported to date are the fourth stream of migrating cranial NCCs observed in the veiled

chameleon[9] (also found in an alligator and an ostrich)[16] and the late wave of trunk NCCs taking a ventromedial (instead of the expected dorsolateral route), which was found in the Californian kingsnake.[7] Our observations in the common wall lizard do not clearly identify a fourth stream of cranial NCCs. However, to confidently rule out the existence of this stream, further analyses including cell lineage tracing may be required. Regarding the ventromedial route of late wave trunk NCCs, we do find ventromedial intra-somitic migration that is coinciding with dorsolateral migration, but it is not clear that these correspond to the late wave ventromedial migration reported for the California kingsnake.[7]

In summary, our study provides the first complete description of NCCs, including cranial, vagal and trunk NCCs, in a lacertid and contributes to our understanding of taxon-specific differences in the regulation of this dynamic cell type. Thus, it lays the foundation for future work targeting the role of this cell type in evolutionary diversifications.

Experimental procedures

Embryo collection

All embryos stem from captive breeding colonies of common wall lizards that were wild caught in central Italy. Parents show variation in phenotypes (coloration, morphology, and behavior), including in traits derived from the neural crest. In the present study, we describe broad developmental patterns that we do not expect to differ on a population level, and we therefore do not discriminate between embryos of different parental origins.

Adult wall lizards were kept as described in Feiner et al., (2018).[87] Eggs were collected during the breeding seasons (April-July) of 2021 to 2023. Each cage had a pot filled with moist sand in which females laid their clutches. The eggs were collected each morning, and one egg per

clutch was dissected immediately to determine the developmental stage (somite count) of the embryos in the clutch. The rest of the eggs were incubated at 24°C in moist vermiculite until the appropriate stage was reached. We aimed to sample a distribution of stages from as young as possible up to around 60ss. Based on 563 eggs, the mean embryonic stage on the day of oviposition was estimated to be 21.4ss (sd = 5.2 somites) and the earliest embryos were at 11ss. The pace of somite formation is constant and has previously been estimated to be four somites per day when incubated at 24°C.[87]

Egg dissections were performed in cold, nuclease-free PBS (10mmol/L phosphate buffer, 2.7mmol/L KCl and 137mmol/L NaCl, pH 7.4) after which each embryo was immediately transferred to 4% paraformaldehyde in PBS for overnight fixation at 4°C on a rotating platform. After fixation, embryos were transferred to gradually increasing concentrations of methanol and stored in 100% methanol at -20°C. A small subset of embryos intended to be used in probe synthesis (see below) was dissected as described above, incubated in RNAlater (Invitrogen AM7020) at 4°C for 24h and then transferred to -80°C for storage.

Immunohistochemistry

Paraformaldehyde-fixed embryos were rehydrated in PBS-T with decreasing concentrations of methanol. Embryos were blocked using TN-blocking buffer with bovine serum albumin (1% bovine serum albumin, 0.1mol/L Tris pH7.5, 0.15 mol/L NaCl in H_2O) followed by overnight incubation with primary antibodies against HNK-1 (1:500; Anti-Hu CD57 eBioscience 11-057742) in TN-blocking buffer. Embryos were washed with PBS and incubated overnight with secondary antibodies (1:200; Alexa Flour 488 goat anti-mouse IgM (μ chain) Invitrogen A21042) in TN-blocking buffer. Embryos were washed in PBS and stained with DAPI (1:500;

ThermoScientific 62248). Lastly, embryos were cleared by overnight incubation in RapiClear 1.49 (SUNJin Lab) and then mounted in fresh RapiClear medium between two 0.17µm cover slips using iSpacers (SUNJin Lab). The stained and cleared embryos were imaged using a confocal microscope (Leica TCS SP8) using a 20X/0.75 IMM objective (plan apochromatic multi-immersion). Tiles were merged and 2D images were rendered using the LAS X software version 0.5.7.23225.

Probe synthesis for *in situ* hybridization

Total RNA was extracted from the RNAlater-stored embryos using the RNeasy Mini Kit (Qiagen) including DNase digestion and stored in nuclease-free water at -80°C. Extracted RNA was used as template in reverse transcription into cDNA using SuperScript III Reverse Transcriptase and oligo-dT primers following the manufacturer's instructions. The selected marker genes were amplified by polymerase chain reaction (PCR) from the cDNA using GoTaq G2 Hot Start Green Master Mix (Promega), and primers designed using the PodMur_1.0 reference genome.[88] Primers were designed to amplify 800-1200 bp of the gene of interest with approximately 500 bps in the 3´UTR and T7 and SP6 promoters attached to the reverse and forward primers, respectively (see Table 1 for primer sequences). Amplified gene fragments were Sanger-sequenced to confirm each amplicon's identity. PCR products were purified using the MinElute PCR Purification Kit (Qiagen) and *in vitro* transcribed to produce antisense RNA-probes using the DIG Probe Synthesis Kit (Roche). The resulting RNA-probes were purified using the RNeasy Mini Kit (Qiagen) and stored in nuclease-free water at -80°C.

Table 1 Sequences of primers used in this study (5' to 3').

Gene	Forward primer	Reverse primer
Snai2	ATAAGCAGTTGCACTGTG	GTGTGTATCAAGCATGTG
Eya2	GATGGTGTTGAAGAGGAA	AGGTAACTCTTTCTCCTG
FoxD3	AAAGCCTTCAACTCCCAG	CTCCCAATCCTTTGCTTG
Mitf	ACCATCACTTTCAACGAC	TTAGAAGGTTGTCCACTC
Snai1	AACTGTGAGAAGGAGTAC	CAAGAGAGAATTGAGTGG
Sox9	AGTTTGACCAGTATCTCC	TAAGGCATGCCATTTTGC
Sox10	AAAGACAGAACTGCAGTC	GAGGGTCGTATATACAG
Th	ATAATATCCCTCAGCTGG	TGGATAGCAACACAAACC
Twist1	TACATCGACTTCCTCTAC	AAATGAAAGAGGAGCAGG
Wnt1	CTCTGCAAGAATAGGAAC	TCATCTACGGCAACAAAG

Whole mount *in situ* hybridization

Following the methodology in Feiner (2019)[89] paraformaldehyde-fixed embryos were rehydrated in nuclease-free PBS-T (1x PBS with 0.1% Tween-20) using gradually lower concentrations of methanol. Embryos were permeabilized using Proteinase K, followed by refixation using 4% paraformaldehyde in PBS. Hybridization was done with 100 ng/mL probe at 68°C in hybridization buffer (5x SSC pH 7.5, 50% deionized formamide, 50 µg/ml heparin, 0.3 mg/ml torula RNA, 2% Tween-20, 2% blocking reagent and 10 mmol/L EDTA). Hybridized embryos were blocked in blocking buffer (1.5% blocking reagent in PBS-T), followed by incubation with 0.1875 U/mL anti-DIG antibody in blocking buffer. This was followed by 1.5 days of washes in maleic acid buffer (15 mmol/L maleic acid pH7.5, 300 mmol/L NaCl and 0.1% Tween-20) before color development with 2% NBT/BCIP in alkaline phosphatase buffer (0.1 mol/L Tris Base pH 9.5, 0.1mol/L NaCl, 1 mmol/L $MgCl_2$ and 0.1% Tween-20). Once a good signal-to-noise ratio was achieved, the

reaction was stopped by extensive washes in PBS-T and re-fixing in 4% paraformaldehyde. Some stained embryos were cross-sectioned by hand using a scalpel. Stained embryos and sections were photographed in glycerol using a Nikon SMZ18 stereo microscope with a Nikon SHR Plan Apo 2X WD: 20 objective and Nikon DS-Ri1 camera.

Gene orthology

Since the orthology relationships of *Snai1* and *Snai2* to other tetrapod genes was unclear[66] a gene tree was constructed to confirm their identities. Both sequences from the common wall lizard were obtained from Ensemble and blasted (protein blast) against the Human, mouse, and chicken databases on NCBI, the top hits were retrieved. Alignment (using the muscle algorithm), model selection (JTT+G) and maximum likelihood tree construction was performed in MEGA.[90]

Reagent list

Reagent	**Company**	**Catalog#**	**Cas#**
PBS	Sigma	P4417	
Water, nucl. free, Mol. Biol. Grade, Ultrapure	ThermoScientific	J71786.K8	
Paraformaldehyde	Sigma-Aldrich	P6148	30525-89-4
Methanol	Merck Millipore	1.06009.1000	67-56-1
RNAlater	Invitrogen	AM7020	
Tween-20	Sigma	P9416	
Tris Base for molecular biology white crystals or powder	Fisher Scientific	BP152	77-86-1
Sodium Chloride, molecular biology grade (NaCl)	MP	194848	7647-14-5
Bovine Serum Albumin (BSA)	Sigma	A9418	

Primary antibody: CD57 Monoclonal Antibody (TB01 (TBO1)), FITC	eBioscience	11-0577-42	
Secondary antibody: Alexa Fluor 488 goat anti-mouse IgM (u chain)	Invitrogen	A21042	
DAPI	ThermoScientific	62248	
RapiClear 1.49	SUNJin Lab	RC149001	
Cover Glass 1.5 (~0.17µm)	VWR	631-0134	
iSpacer	SUNJin Lab		
Rneasy Mini Kit	Qiagen	74104	
SupersScript III Reverse Transcriptase	Invitrogen	18080	
GoTaq G2 Hot Start Green Master Mix	Promega	M742A	
MinElute PCR Purification Kit	Qiagen	28004	
DIG-labeled dNTPs	Roche	1.16E+10	
Proteinase K, recombinant PCR Grade	Roche	3.12E+09	
20x SSC	Fisher BioReagents	BP13254	
Formamide deionized for mol. Biology	PanReac AppliChem	A2156	1975-12-07
Heparin sodium salt from porcine intestinal mucosa	Sigma-Aldrich	H4784	9041-08-01
Riobonucleic acid from torula yeast	Sigma	R6625	63231-63-0
Blocking Reagent	Roche	1.11E+10	
EDTA	Invitrogen	AM9260G	
Anti-Digoxenin-AP Fab fragments	Roche	1.11E+10	
Maleic acid	Sigma-Aldrich	M0375	110-16-7
NBT/BCIP	Roche	1.17E+10	
Glycerol	VWR	24397.3	56-81-5

Acknowledgements

We are grateful to Stanley Heinze, Michael Bok, Marjorie Lienard and Carina Rasmussen for technical advice and Ola Gustafsson for help with confocal microscopy. We thank Tobias Uller for valuable discussion and help with animal husbandry.

References

1. Barresi MJF, Gilbert SF. *Developmental Biology*. 12th ed. Oxford, New York: Oxford University Press; 2020.

2. Alkobtawi M, Monsoro-Burq AH. The neural crest, a vertebrate invention. In: *Evolving Neural Crest Cells*. Evolutionary cell biology. Boca Raton: CRC Press; 2020:5-66. DOI: 10.1201/b22096

3. Abitua PB. The Hunt for Neural Crest in Invertebrate Chordates. In: *Evolving Neural Crest Cells*. Evolutionary cell biology. Boca Raton: CRC Press; 2020:137-156. https://doi.org/10.1201/b22096

4. Kuratani S. Neural Crest and Craniofacial Evolution of Early Vertebrates. In: *Evolving Neural Crest Cells*. Evolutionary cell biology. Boca Raton: CRC Press; 2020:185-218. https://doi.org/10.1201/b22096

5. Yu JK, Su YH. The Evolution of the Neural Border and Peripheral Nervous System—Insights from Invertebrate Deuterostome Animals. In: *Evolving Nerual Crest Cells*. Evolutionary cell biology. Boca Raton: CRC Press; 2020:103-136. https://doi.org/10.1201/b22096

6. Cerrizuela S, Vega-Lopez GA, Méndez-Maldonado K, Velasco I, Aybar MJ. The crucial role of model systems in understanding the complexity of cell signaling in human neurocristopathies. *WIREs Mechanisms of Disease*. 2022;14(1):e1537. https://doi.org/10.1002/wsbm.1537

7. Reyes M, Zandberg K, Desmawati I, De Bellard ME. Emergence and migration of trunk neural crest cells in a snake, the California Kingsnake (Lampropeltis getula californiae). *BMC Developmental Biology*. 2010;10. https://doi.org/10.1186/1471-213X-10-52

8. Khannoon ER, Alvarado C, Poveda R, de Bellard ME. Description of trunk neural crest migration and peripheral nervous system formation in the Egyptian cobra Naja haje haje. *Differentiation*. 2023;133:40-50. https://doi.org/10.1016/j.diff.2023.06.002

9. Diaz RE, Shylo NA, Roellig D, Bronner M, Trainor PA. Filling in the phylogenetic gaps: Induction, migration, and differentiation of neural crest cells in a squamate reptile, the

veiled chameleon (Chamaeleo calyptratus). *Developmental Dynamics*. 2019;248(8):709-727. https://doi.org/10.1002/dvdy.38

10. Nichols DH. Neural crest formation in the head of the mouse embryo as observed using a new histological technique. *Development*. 1981;64(1):105-120. https://doi.org/10.1242/dev.64.1.105

11. Nichols DH. Formation and distribution of neural crest mesenchyme to the first pharyngeal arch region of the mouse embryo. *American Journal of Anatomy*. 1986;176(2):221-231. https://doi.org/10.1002/aja.1001760210

12. Serbedzija GN, Bronner-Fraser M, Fraser SE. Vital dye analysis of cranial neural crest cell migration in the mouse embryo. *Development*. 1992;116(2):297-307. https://doi.org/10.1242/dev.116.2.297

13. O'Rahilly R, Müller F. The development of the neural crest in the human. *Journal of Anatomy*. 2007;211(3):335-351. https://doi.org/10.1111/j.1469-7580.2007.00773.x

14. Le Douarin N, Kalcheim C. *The Neural Crest*. 2nd ed.; 1999. Accessed May 2, 2024. https://www.cambridge.org/se/academic/subjects/life-sciences/cell-biology-and-developmental-biology/neural-crest-2nd-edition, https://www.cambridge.org/se/academic/subjects/life-sciences/cell-biology-and-developmental-biology

15. Le Douarin NM. The avian embryo as a model to study the development of the neural crest: a long and still ongoing story. *Mechanisms of Development*. 2004;121(9):1089-1102. https://doi.org/10.1016/j.mod.2004.06.003

16. Kundrát M. Heterochronic shift between early organogenesis and migration of cephalic neural crest cells in two divergent evolutionary phenotypes of archosaurs: Crocodile and ostrich. *Evolution and Development*. 2009;11(5):535-546. https://doi.org/10.1111/j.1525-142X.2009.00352.x

17. Bronner-Fraser M. Analysis of the early stages of trunk neural crest migration in avian embryos using monoclonal antibody HNK-1. *Developmental Biology*. 1986;115(1):44-55. https://doi.org/10.1016/0012-1606(86)90226-5

18. Harris ML, Erickson CA. Lineage specification in neural crest cell pathfinding. *Developmental Dynamics*. 2007;236(1):1-19. https://doi.org/10.1002/dvdy.20919

19. Weston JA. 6 Sequential Segregation and Fate of Developmentally Restricted Intermediate Cell Populations in the Neural Crest Lineage. In: Bode HR, ed. *Current Topics in Developmental Biology*. Vol 25. Academic Press; 1991:133-153. https://doi.org/10.1016/S0070-2153(08)60414-7

20. Kuo BR, Erickson CA. Vagal neural crest cell migratory behavior: A transition between the cranial and trunk crest. *Developmental Dynamics*. 2011;240(9):2084-2100. https://doi.org/10.1002/dvdy.22715

21. Brandon AA, Almeida D, Powder KE. Neural crest cells as a source of microevolutionary variation. *Seminars in Cell & Developmental Biology*. Published online June 16, 2022. https://doi.org/10.1016/j.semcdb.2022.06.001

22. Darwin C. *The Variation of Animals and Plants under Domestication*. Vol 2. 2nd ed. London: John Murray; 1888.

23. Wilkins AS, Wrangham RW, Tecumseh Fitch W. The “domestication syndrome” in mammals: A unified explanation based on neural crest cell behavior and genetics. *Genetics*. 2014;197(3):795-808. https://doi.org/10.1534/genetics.114.165423

24. San-Jose LM, Roulin A. On the Potential Role of the Neural Crest Cells in Integrating Pigmentation Into Behavioral and Physiological Syndromes. *Frontiers in Ecology and Evolution*. 2020;8:278. https://doi.org/10.3389/fevo.2020.00278

25. Uller T, Moczek AP, Watson RA, Brakefield PM, Laland KN. Developmental Bias and Evolution: A Regulatory Network Perspective. *Genetics*. 2018;209(4):949-966. https://doi.org/10.1534/genetics.118.300995

26. Böhme W. *Handbuch der Reptilien und Amphibien Europas Band2/II Echsen III (Podarcis)*. Wiesbaden: AULA-Verlag; 1986.

27. Eimer T, Eimer A. *Untersuchungen Über Das Variiren Der Mauereidechse : Ein Beitrag Zur Theorie von Der Entwicklung Aus Constitutionellen Ursachen, Sowie Zum Darwinismus*. Berlin: Nicolaische Verlags-Buchhandlung; 1881. https://doi.org/10.5962/bhl.title.49215

28. Kammerer P. *Der Artenwandel Auf Inseln Und Seine Ursachen Ermittelt Durch Vergleich Und Versuch an Den Eidechsen Der Dalmatinischen Eilande*. Leipzig und Wien: Verlag von Franz Deuticke; 1926.

29. While GM, Michaelides S, Heathcote RJP, et al. Sexual selection drives asymmetric introgression in wall lizards. *Ecology Letters*. 2015;18(12):1366-1375. https://doi.org/10.1111/ele.12531

30. Miñano MR, While GM, Yang W, et al. Climate Shapes the Geographic Distribution and Introgressive Spread of Color Ornamentation in Common Wall Lizards. *The American Naturalist*. 2021;198(3):379-393. https://doi.org/10.1086/715186

31. Yang W, While GM, Laakkonen H, et al. Genomic evidence for asymmetric introgression by sexual selection in the common wall lizard. *Molecular Ecology*. 2018;27(21):4213-4224. https://doi.org/10.1111/mec.14861

32. Feiner N, Yang W, Bunikis I, While GM, Uller T. Adaptive introgression reveals the genetic basis of a sexually selected syndrome in wall lizards. *Science Advances*. 2024;10(14):eadk9315. https://doi.org/10.1126/sciadv.adk9315

33. Heathcote RJP, While GM, MacGregor HEA, et al. Male behaviour drives assortative reproduction during the initial stage of secondary contact. *Journal of Evolutionary Biology*. 2016;29(5):1003-1015. https://doi.org/10.1111/jeb.12840

34. MacGregor HEA, While GM, Barrett J, et al. Experimental contact zones reveal causes and targets of sexual selection in hybridizing lizards. *Functional Ecology*. 2017;31(3):742-752. https://doi.org/10.1111/1365-2435.12767

35. Nagase T, Sanai Y, Nakamura S, Asato H, Harii K, Osumi N. Roles of HNK-1 carbohydrate epitope and its synthetic glucuronyltransferase genes on migration of rat neural crest cells. *Journal of Anatomy*. 2003;203(1):77-88. https://doi.org/10.1046/j.1469-7580.2003.00205.x

36. Bronner-Fraser M. Perturbation of cranial neural crest migration by the HNK-1 antibody. *Developmental Biology*. 1987;123(2):321-331. https://doi.org/10.1016/0012-1606(87)90390-3

37. Clark K, Bender G, Murray BP, et al. Evidence for the neural crest origin of turtle plastron bones. *genesis*. 2001;31(3):111-117. https://doi.org/10.1002/gene.10012

38. Giovannone D, Ortega B, Reyes M, et al. Chicken trunk neural crest migration visualized with HNK1. *Acta Histochemica*. 2015;117(3):255-266. https://doi.org/10.1016/j.acthis.2015.03.002

39. Hirata M, Ito K, Tsuneki K. Migration and Colonization Patterns of HNK-1-Immunoreactive Neural Crest Cells in Lamprey and Swordtail Embryos. *jzoo*. 1997;14(2):305-312. https://doi.org/10.2108/zsj.14.305

40. Juarez M, Reyes M, Coleman T, et al. Characterization of the trunk neural crest in the bamboo shark, Chiloscyllium punctatum. *Journal of Comparative Neurology*. 2013;521(14):3303-3320. https://doi.org/10.1002/cne.23351

41. Kalcheim C, Le Douarin NM. Requirement of a neural tube signal for the differentiation of neural crest cells into dorsal root ganglia. *Developmental Biology*. 1986;116(2):451-466. https://doi.org/10.1016/0012-1606(86)90146-6

42. Olsson L, Moury JD, Carl TF, Håstad O, Hanken J. Cranial neural crest-cell migration in the direct-developing frog, Eleutherodactylus coqui: Molecular heterogeneity within and among migratory streams. *Zoology*. 2002;105(1):3-13. https://doi.org/10.1078/0944-2006-00051

43. Erickson CA, Loring JF, Lester SM. Migratory pathways of HNK-1-immunoreactive neural crest cells in the rat embryo. *Developmental Biology*. 1989;134(1):112-118. https://doi.org/10.1016/0012-1606(89)90082-1

44. Tucker GC, Delarue M, Zada S, Boucaut JC, Thiery JP. Expression of the HNK-1/NC-1 epitope in early vertebrate neurogenesis. *Cell Tissue Res*. 1988;251(2):457-465. https://doi.org/10.1007/BF00215855

45. Abo T, Balch CM. A differentiation antigen of human NK and K cells identified by a monoclonal antibody (HNK-1). *The Journal of Immunology*. 1981;127(3):1024-1029. https://doi.org/10.4049/jimmunol.127.3.1024

46. Simões-Costa M, Bronner ME. Establishing neural crest identity: a gene regulatory recipe. *Development (Cambridge, England)*. 2015;142(2):242-257. https://doi.org/10.1242/dev.105445

47. Qin Q, Xu Y, He T, Qin C, Xu J. Normal and disease-related biological functions of Twist1 and underlying molecular mechanisms. *Cell Res*. 2012;22(1):90-106. https://doi.org/10.1038/cr.2011.144

48. Soldatov R, Kaucka M, Kastriti ME, et al. Spatiotemporal structure of cell fate decisions in murine neural crest. *Science*. 2019;364(6444):eaas9536. https://doi.org/10.1126/science.aas9536

49. Howard AG, Baker PA, Ibarra-García-Padilla R, et al. An atlas of neural crest lineages along the posterior developing zebrafish at single-cell resolution. *eLife*. 2021;10:1-31. https://doi.org/10.7554/eLife.60005

50. Hanemaaijer ES, Margaritis T, Sanders K, et al. Single-cell atlas of developing murine adrenal gland reveals relation of Schwann cell precursor signature to neuroblastoma phenotype. *PNAS*. 2021;118(5). https://doi.org/10.1073/pnas.2022350118

51. Kuratani SC, Kirby ML. Initial migration and distribution of the cardiac neural crest in the avian embryo: An introduction to the concept of the circumpharyngeal crest. *American Journal of Anatomy*. 1991;191(3):215-227. https://doi.org/10.1002/aja.1001910302

52. Kvasilova A, Gregorovicova M, Kundrat M, Sedmera D. HNK-1 in Morphological Study of Development of the Cardiac Conduction System in Selected Groups of Sauropsida. *The Anatomical Record*. 2019;302(1):69-82. https://doi.org/10.1002/ar.23925

53. Nakagawa M, Thompson RP, Terracio L, Borg TK. Developmental anatomy of HNK-1 immunoreactivity in the embryonic rat heart: co-distribution with early conduction tissue. *Anat Embryol*. 1993;187(5):445-460. https://doi.org/10.1007/BF00174420

54. Chuck ET, Watanabe M. Differential expression of PSA-NCAM and HNK-1 epitopes in the developing cardiac conduction system of the chick. *Developmental Dynamics*.

1997;209(2):182-195. https://doi.org/10.1002/(SICI)1097-0177(199706)209:2<182::AID-AJA4>3.0.CO;2-E

55. Ikeda T, Iwasaki K, Shimokawa I, Sakai H, Ito H, Matsuo T. Leu-7 immunoreactivity in human and rat embryonic hearts, with special reference to the development of the conduction tissue. *Anat Embryol*. 1990;182(6):553-562. https://doi.org/10.1007/BF00186462

56. Freyer L, Aggarwal V, Morrow BE. Dual embryonic origin of the mammalian otic vesicle forming the inner ear. *Development*. 2011;138(24):5403-5414. https://doi.org/10.1242/dev.069849

57. Lee VM, Sechrist JW, Luetolf S, Bronner-Fraser M. Both neural crest and placode contribute to the ciliary ganglion and oculomotor nerve. *Developmental Biology*. 2003;263(2):176-190. https://doi.org/10.1016/j.ydbio.2003.07.004

58. Streeter GL. The development of the cranial and spinal nerves in the occipital region of the human embryo. *American Journal of Anatomy*. 1905;4(1):83-116. https://doi.org/10.1002/aja.1000040106

59. Goldberg S, Venkatesh A, Martinez J, et al. The development of the trunk neural crest in the turtle Trachemys scripta. *Developmental Dynamics*. 2020;249(1):125-140. https://doi.org/10.1002/dvdy.119

60. Canning CA, Lee L, Irving C, Mason I, Jones CM. Sustained interactive Wnt and FGF signaling is required to maintain isthmic identity. *Developmental Biology*. 2007;305(1):276-286. https://doi.org/10.1016/j.ydbio.2007.02.009

61. Nothwang HG, Ebbers L, Schlüter T, Willaredt MA. The emerging framework of mammalian auditory hindbrain development. *Cell Tissue Res*. 2015;361(1):33-48. https://doi.org/10.1007/s00441-014-2110-7

62. Azambuja AP, Simoes-Costa M. A regulatory sub-circuit downstream of Wnt signaling controls developmental transitions in neural crest formation. *PLOS Genetics*. 2021;17(1):e1009296. https://doi.org/10.1371/journal.pgen.1009296

63. Yoshida T, Vivatbutsiri P, Morriss-Kay G, Saga Y, Iseki S. Cell lineage in mammalian craniofacial mesenchyme. *Mechanisms of Development*. 2008;125(9):797-808. https://doi.org/10.1016/j.mod.2008.06.007

64. Chai Y, Jiang X, Ito Y, et al. Fate of the mammalian cranial neural crest during tooth and mandibular morphogenesis. *Development*. 2000;127(8):1671-1679. https://doi.org/10.1242/dev.127.8.1671

65. Barrallo-Gimeno A, Nieto MA. The Snail genes as inducers of cell movement and survival: implications in development and cancer. *Development*. 2005;132(14):3151-3161. https://doi.org/10.1242/dev.01907

66. Sefton M, Sanchez S, Nieto MA. Conserved and divergent roles for members of the Snail family of transcription factors in the chick and mouse embryo. *Development*. 1998;125(16):3111-3121. https://doi.org/10.1242/dev.125.16.3111

67. Barriga EH, Maxwell PH, Reyes AE, Mayor R. The hypoxia factor Hif-1α controls neural crest chemotaxis and epithelial to mesenchymal transition. *Journal of Cell Biology*. 2013;201(5):759-776. https://doi.org/10.1083/jcb.201212100

68. Vincentz JW, Firulli BA, Lin A, Spicer DB, Howard MJ, Firulli AB. Twist1 Controls a Cell-Specification Switch Governing Cell Fate Decisions within the Cardiac Neural Crest. *PLOS Genetics*. 2013;9(3):e1003405. https://doi.org/10.1371/journal.pgen.1003405

69. Tavares AT, Izpisuja-Belmonte JC, Rodriguez-Leon J. Developmental expression of chick twist and its regulation during limb patterning. *Int J Dev Biol*. 2004;45(5-6):707-713. https://doi.org/10.1387/ijdb.11669372

70. Liu JAJ, Wu MH, Yan CH, et al. Phosphorylation of Sox9 is required for neural crest delamination and is regulated downstream of BMP and canonical Wnt signaling. *Proceedings of the National Academy of Sciences*. 2013;110(8):2882-2887. https://doi.org/10.1073/pnas.1211747110

71. McKeown SJ, Lee VM, Bronner-Fraser M, Newgreen DF, Farlie PG. Sox10 overexpression induces neural crest-like cells from all dorsoventral levels of the neural tube but inhibits differentiation. *Developmental Dynamics*. 2005;233(2):430-444. https://doi.org/10.1002/dvdy.20341

72. Kos R, Reedy MV, Johnson RL, Erickson CA. The winged-helix transcription factor FoxD3 is important for establishing the neural crest lineage and repressing melanogenesis in avian embryos. *Development*. 2001;128(8):1467-1479. https://doi.org/10.1242/dev.128.8.1467

73. Lukoseviciute M, Gavriouchkina D, Williams RM, et al. From Pioneer to Repressor: Bimodal foxd3 Activity Dynamically Remodels Neural Crest Regulatory Landscape In Vivo. *Developmental Cell*. 2018;47(5):608-628.e6. https://doi.org/10.1016/j.devcel.2018.11.009

74. Cheng YC, Cheung M, Abu-Elmagd MM, Orme A, Scotting PJ. Chick Sox10, a transcription factor expressed in both early neural crest cells and central nervous system. *Developmental Brain Research*. 2000;121(2):233-241. https://doi.org/10.1016/S0165-3806(00)00049-3

75. Zhang T, Xu J, Xu PX. Eya2 expression during mouse embryonic development revealed by Eya2lacZ knockin reporter and homozygous mice show mild hearing loss. *Developmental Dynamics*. 2021;250(10):1450-1462. https://doi.org/10.1002/dvdy.326

76. Bell GW, Yatskievych TA, Antin PB. GEISHA, a whole-mount in situ hybridization gene expression screen in chicken embryos. *Developmental Dynamics*. 2004;229(3):677-687. https://doi.org/10.1002/dvdy.10503

77. Xu PX, Woo I, Her H, Beier DR, Maas RL. Mouse Eya homologues of the Drosophila eyes absent gene require Pax6 for expression in lens and nasal placode. *Development*. 1997;124(1):219-231. https://doi.org/10.1242/dev.124.1.219

78. D'Autréaux F, Coppola E, Hirsch MR, Birchmeier C, Brunet JF. Homeoprotein Phox2b commands a somatic-to-visceral switch in cranial sensory pathways. *Proceedings of the National Academy of Sciences*. 2011;108(50):20018-20023. https://doi.org/10.1073/pnas.1110416108

79. Furlan A, Dyachuk V, Kastriti ME, et al. Multipotent peripheral glial cells generate neuroendocrine cells of the adrenal medulla. *Science*. 2017;357(6346):eaal3753. https://doi.org/10.1126/science.aal3753

80. Pattyn A, Morin X, Cremer H, Goridis C, Brunet JF. The homeobox gene Phox2b is essential for the development of autonomic neural crest derivatives. *Nature*. 1999;399(6734):366-370. https://doi.org/10.1038/20700

81. Patthey C, Clifford H, Haerty W, Ponting CP, Shimeld SM, Begbie J. Identification of molecular signatures specific for distinct cranial sensory ganglia in the developing chick. *Neural Development*. 2016;11(3). https://doi.org/10.1186/s13064-016-0057-y

82. Pattyn A, Morin X, Cremer H, Goridis C, Brunet JF. Expression and interactions of the two closely related homeobox genes Phox2a and Phox2b during neurogenesis. *Development*. 1997;124(20):4065-4075. https://doi.org/10.1242/dev.124.20.4065

83. Chan WH, Komada M, Fukushima T, Southard-Smith EM, Anderson CR, Wakefield MJ. RNA-seq of Isolated Chromaffin Cells Highlights the Role of Sex-Linked and Imprinted Genes in Adrenal Medulla Development. *Sci Rep*. 2019;9(1):3929. https://doi.org/10.1038/s41598-019-40501-0

84. Khannoon T, Alvarado C, De Bellard ME. Early Development of The Trunk Neural Crest Cells in the Egyptian Cobra Naja H. Haje. Published online May 26, 2021. https://doi.org/10.21203/rs.3.rs-547365/v1

85. Kundrát M. HNK-1 immunoreactivity during early morphogenesis of the head region in a nonmodel vertebrate, crocodile embryo. *Naturwissenschaften*. 2008;95(11):1063-1072. https://doi.org/10.1007/s00114-008-0426-4

86. Atkins N, Jones SM, Guillette LJ. Timing of parturition in two species of viviparous lizard: influences of β-adrenergic stimulation and temperature upon uterine responses to arginine vasotocin (AVT). *J Comp Physiol B*. 2006;176(8):783-792. https://doi.org/10.1007/s00360-006-0100-0

87. Feiner N, Rago A, While GM, Uller T. Signatures of selection in embryonic transcriptomes of lizards adapting in parallel to cool climate. *Evolution*. 2018;72(1):67-81. https://doi.org/10.1111/evo.13397

88. Andrade P, Pinho C, Pérez i de Lanuza G, et al. Regulatory changes in pterin and carotenoid genes underlie balanced color polymorphisms in the wall lizard. *Proceedings of the National Academy of Sciences*. 2019;116(12):5633-5642. https://doi.org/10.1073/pnas.1820320116

89. Feiner N. Evolutionary lability in Hox cluster structure and gene expression in Anolis lizards. *Evolution Letters*. 2019;3(5):474-484. https://doi.org/10.1002/evl3.131

90. Tamura K, Stecher G, Kumar S. MEGA11: Molecular Evolutionary Genetics Analysis Version 11. *Molecular Biology and Evolution*. 2021;38(7):3022-3027. https://doi.org/10.1093/molbev/msab120